Modeling and Analysis of Seismogram Envelopes in Short Periods

Haruo SATO
Tohoku University, Sendai, Japan

- Coda waves of local earthquakes
- Random heterogeneities seen in well log data
  Random fluctuation, ACF/PSDF, Power-law spectra
- Scalar wave equation in random media
  Born app., Scattering coefficient
- Radiative transfer theory (RTT) in scattering media
  Boltzmann eq.
- Multiple isotropic scattering model for coda excitation
  Measurements of total scattering co. , intrinsic abs., and source energy radiation
- Nonisotropic scattering model
  Spherical harmonics expansion method, Monte Carlo method
- Envelope broadening and Markov approximation method
  Direct derivation of MS envelope based on the parabolic app.
- Model of whole S-envelope from onset to coda (ongoing study)
  Use of the Markov propagator and transport scat. co. in the MIS model
- In this talk, we focus on the scalar wave equation only.

at NRCDP (NIED) in 1974

Seismograms registered at a deep well site IWT:
Direct arrivals+ smoothed envelopes

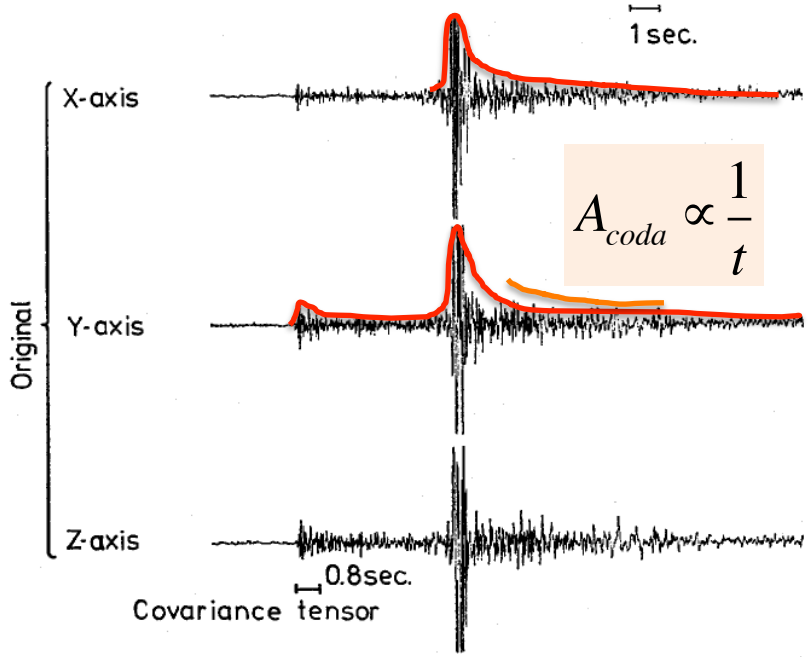

$$A_{coda} \propto \frac{1}{t}$$

How shall we interpret seismogram envelopes in relation with random heterogeneities?

Aki and Chouet, Origin of coda waves, JGR, 1975.

Sonic and density well logs at IWT:
Step like changes + random fluctuation

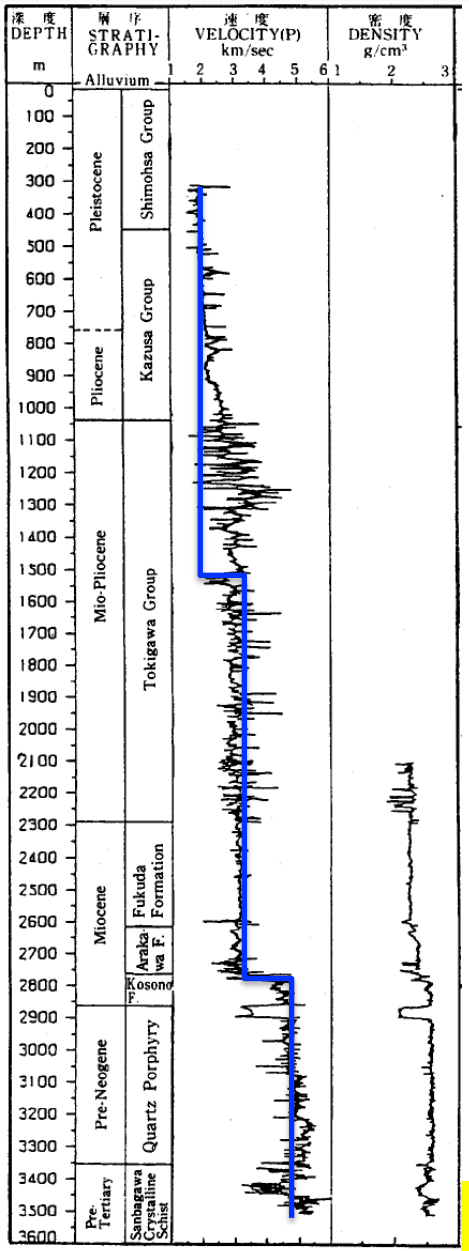

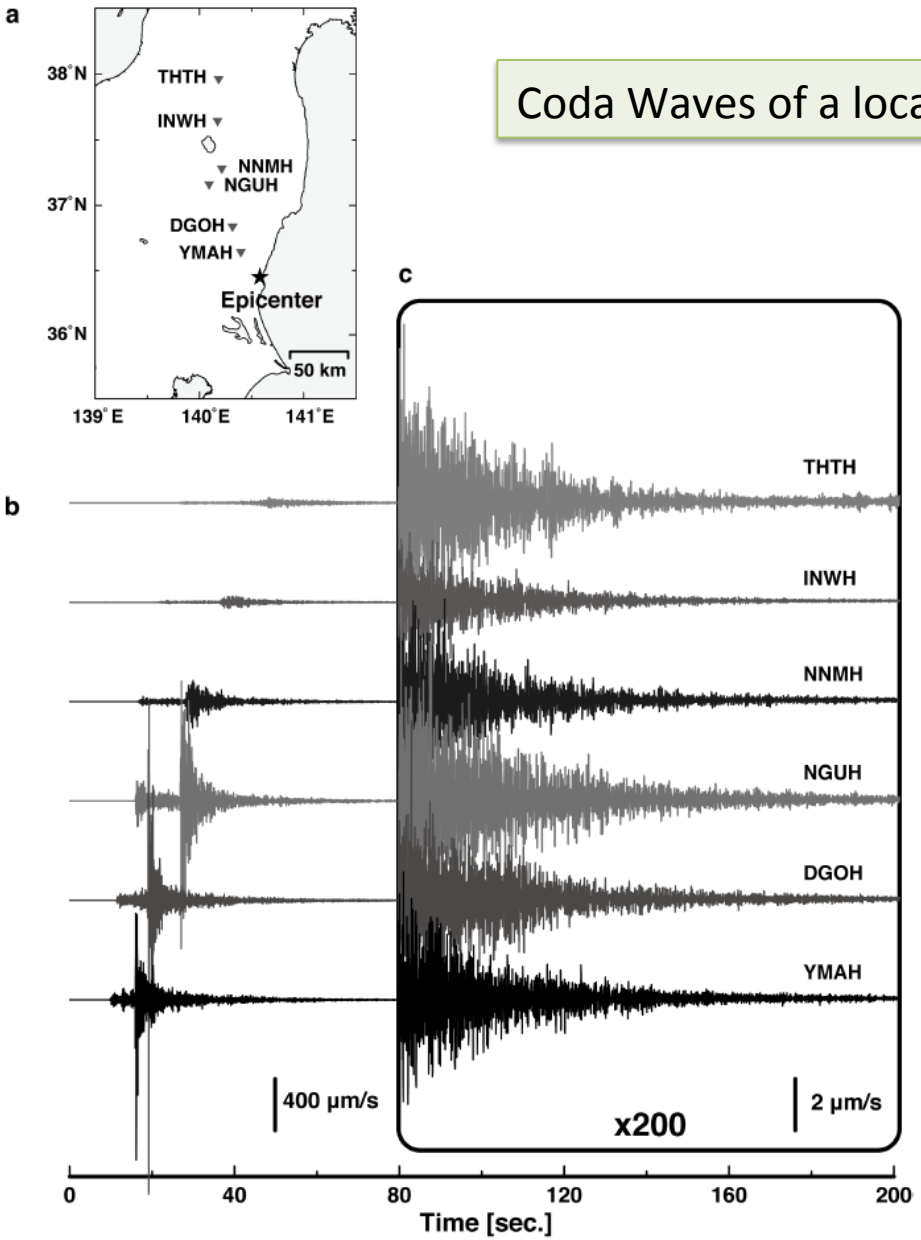

Fig. 1.1 (a) Epicenter (star) of an M_W 4.8 earthquake with 55.3 km in focal depth and Hi-net stations (reversed triangles) of NIED in Honshu, Japan. (b) Velocity seismograms (horizontal transverse component) arranged from bottom to top by increasing epicentral distance, where the gain is the same for all the traces. (c) Magnification of 200 times.

Coda Waves of a local earthquake registered by Hi-net

Common decay curve for coda amplitude envelopes independent of epicentral distances

Courtesy of T. Maeda

F-K Analysis

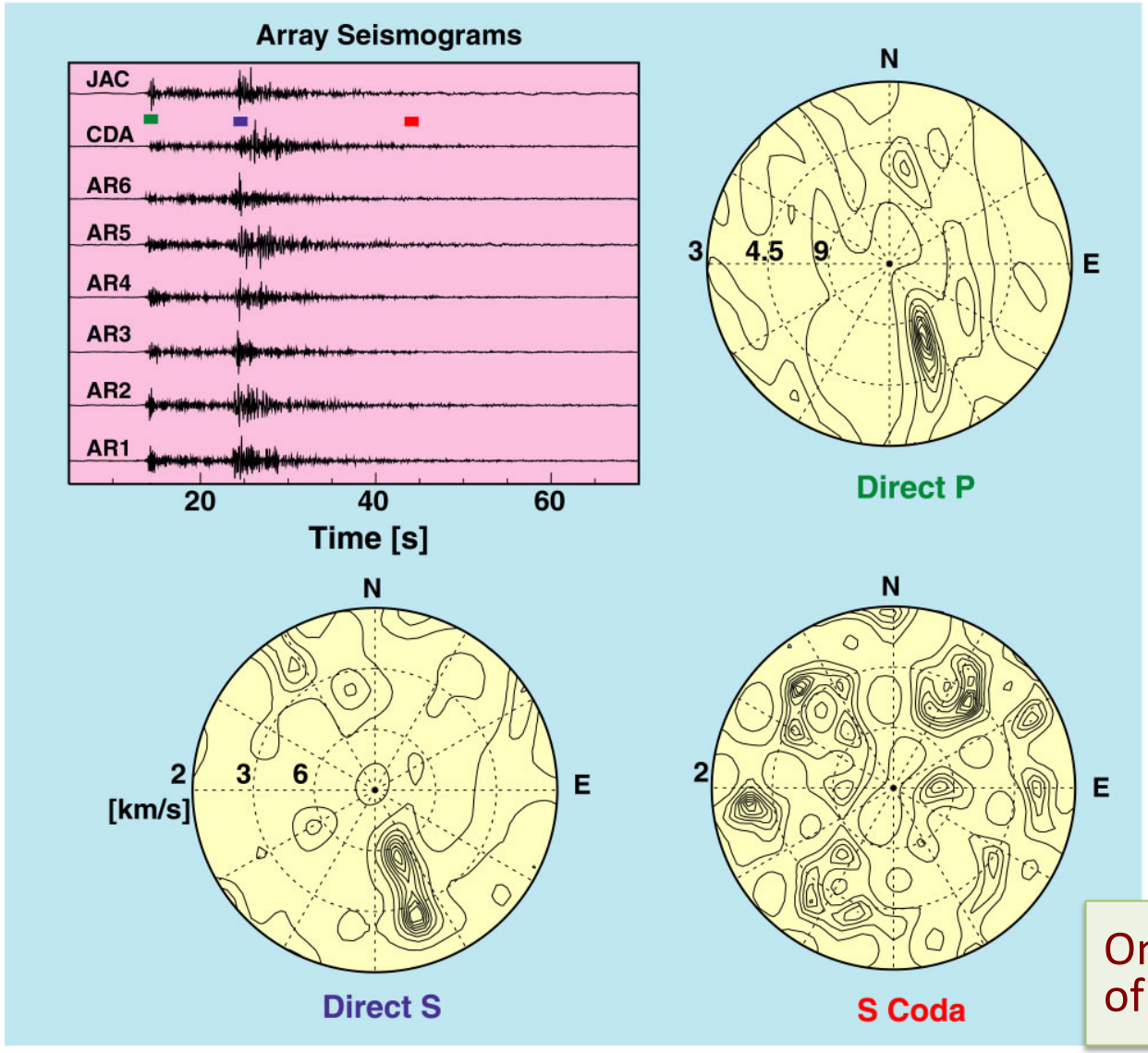

Omni-directional arrivals of S-coda waves

superposition of scattered S-waves

- To focus on amplitude envelope disregarding complex phases
- To study how seismogram envelopes vary with lapse time, travel distance and ray paths in different frequency bands.

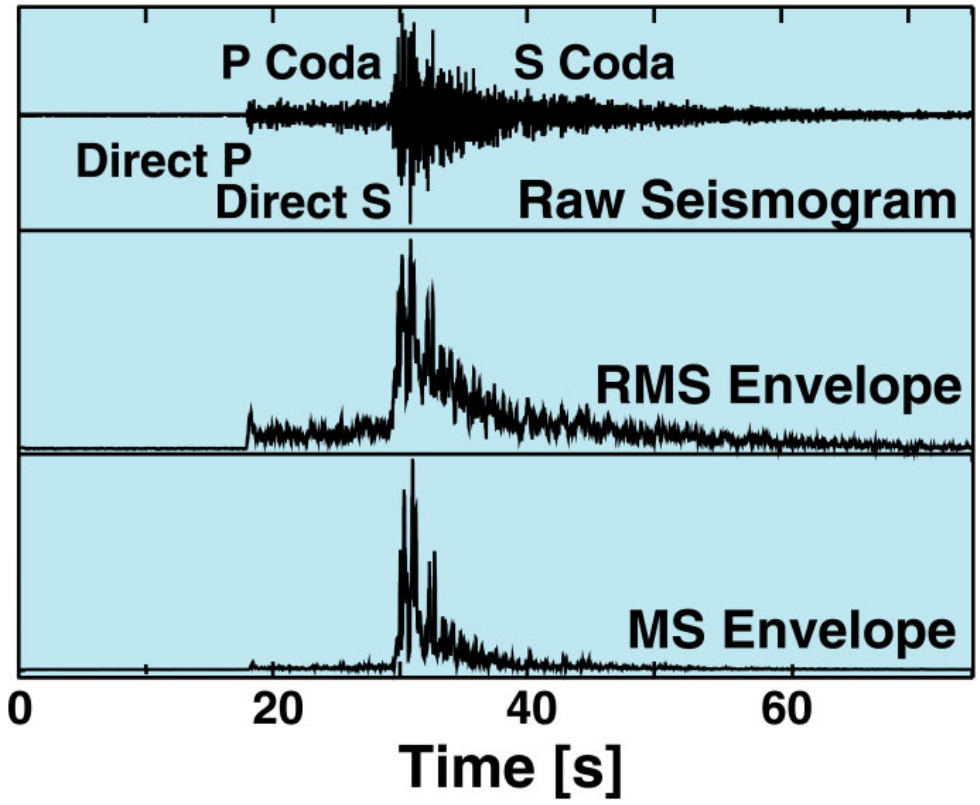

$$E(t, f_c) = \text{MS Amp.}\ (t, f_c, \Delta f)$$

Δf : Octave band width

- Random heterogeneities seen in well log data

ACF/PSDF of fractional fluctuation
of well log data (Volcanic tuff, Kyushu, Japan)

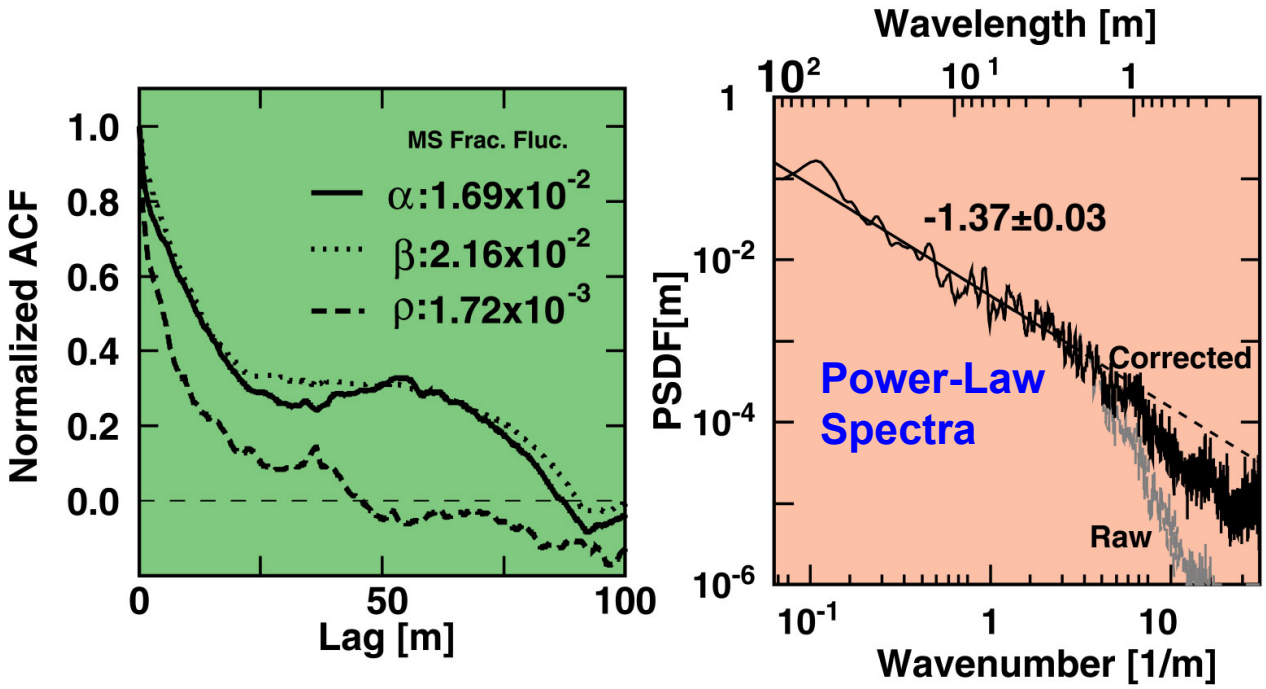

Shiomi et al. [1997]

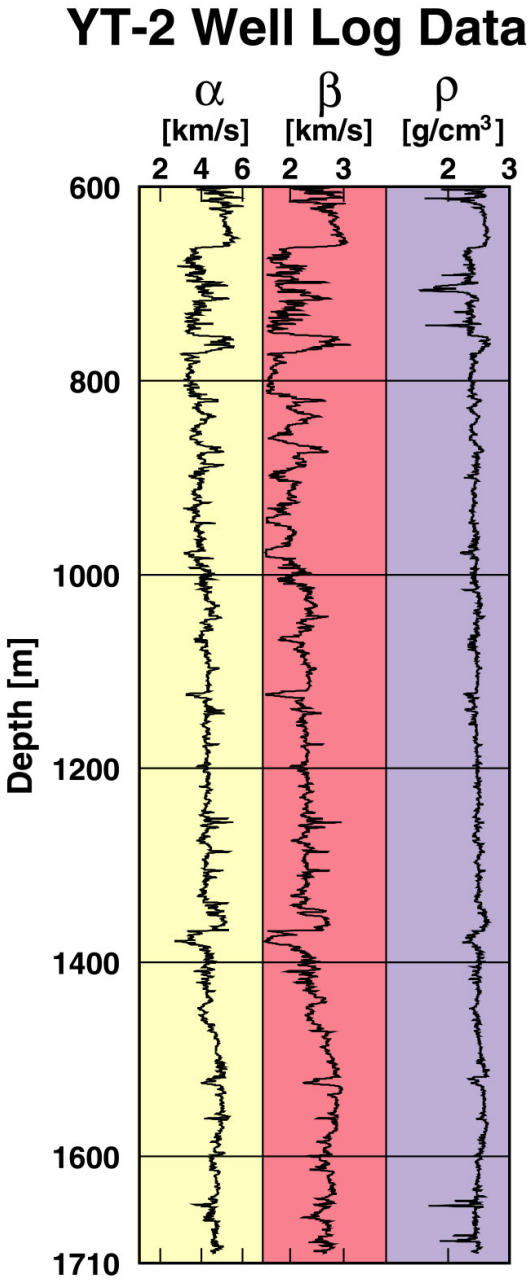

Ensemble of random media

$$V(\mathbf{x}) = V_0 + \delta V(\mathbf{x}) = V_0[1 + \xi(\mathbf{x})],$$

$$R(\mathbf{x}) \equiv \langle \xi(\mathbf{y})\, \xi(\mathbf{y}+\mathbf{x}) \rangle,$$

$$P(\mathbf{m}) = P(m) = \widetilde{R}(\mathbf{x}) = \iiint_{-\infty}^{\infty} R(\mathbf{x})\, e^{-i\mathbf{m}\mathbf{x}} d\mathbf{x},$$

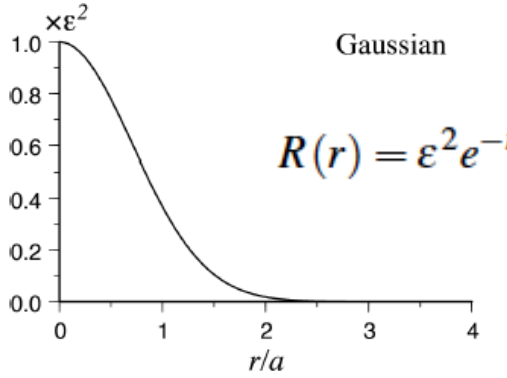

Gaussian

$$R(r) = \varepsilon^2 e^{-r^2/a^2}.$$

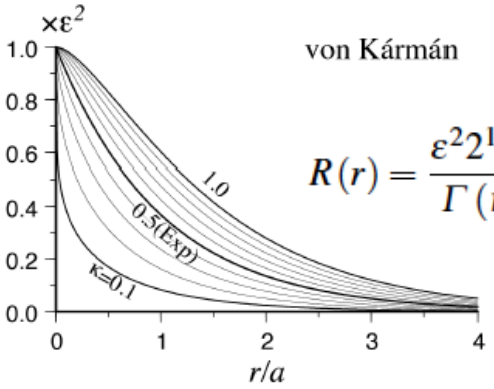

von Kármán

$$R(r) = \frac{\varepsilon^2 2^{1-\kappa}}{\Gamma(\kappa)} \left(\frac{r}{a}\right)^{\kappa} K_{\kappa}\left(\frac{r}{a}\right)$$

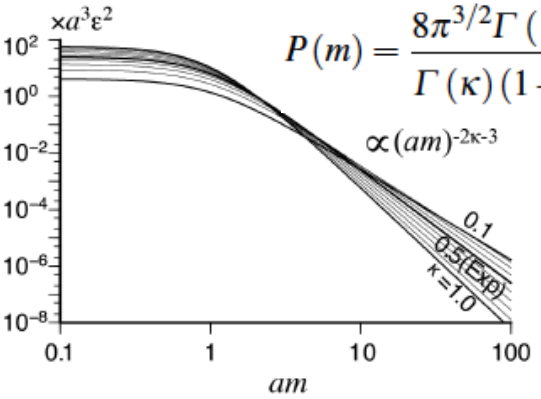

$$P(m) = \frac{8\pi^{3/2}\Gamma(\kappa+3/2)\varepsilon^2 a^3}{\Gamma(\kappa)(1+a^2m^2)^{\kappa+3/2}}$$

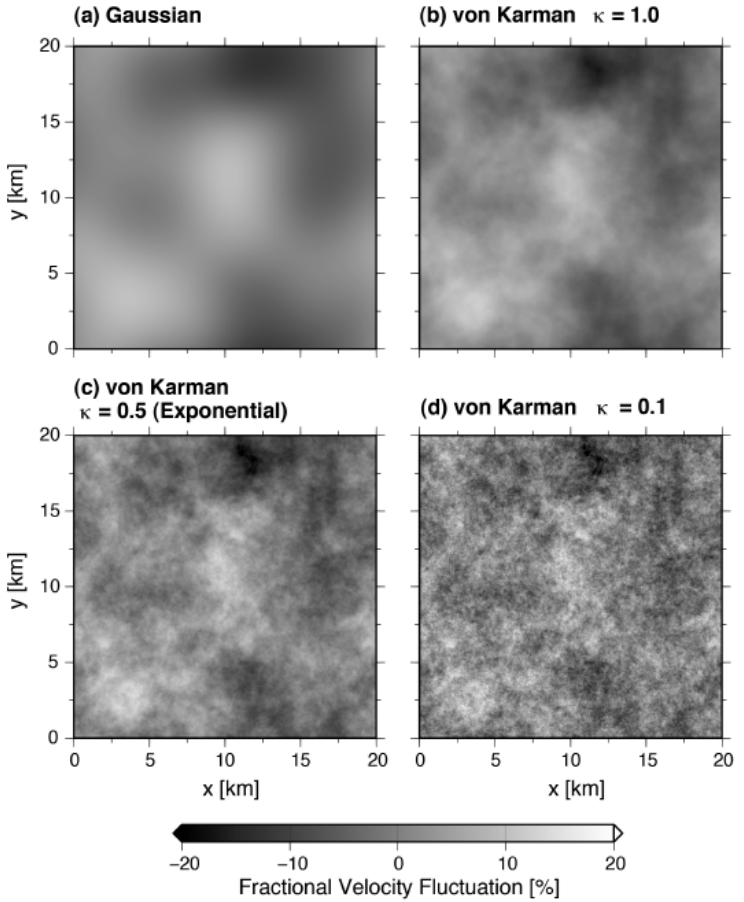

Parameters: RMS fractional fluctuation ε and correlation distance *a*

Scalar wave equation in random media

$$\Delta u - \frac{1}{V_0^2}\partial_t^2 u = -\frac{2}{V_0^2}\xi(\mathbf{x})\partial_t^2 u.$$

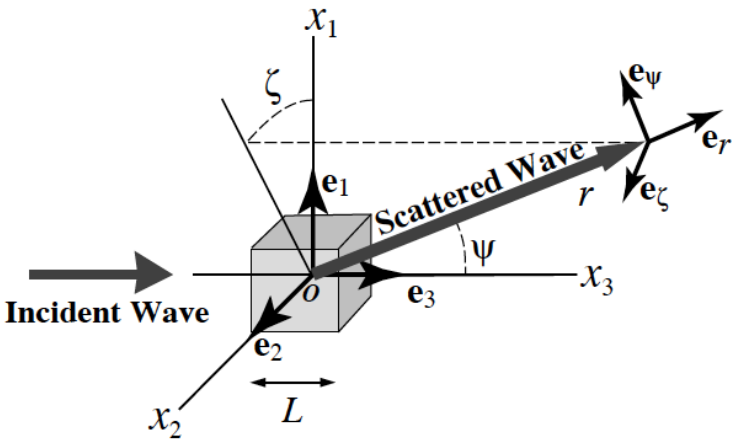

Born approximation

$$u \approx e^{i(k_0 z-\omega t)} + F\frac{e^{i(k_0 r-\omega t)}}{r}$$

$$F = \frac{-k_0^2}{2\pi}\int \xi(\mathbf{x}')e^{-ik_0(\mathbf{e}_r-\mathbf{e}_z)\mathbf{x}'}d\mathbf{x}'$$

Scattering coefficient: Scattering power per unit volume

$$g(\psi;\omega) \equiv 4\pi\frac{1}{L^3}\left\langle\frac{d\sigma}{d\Omega}\right\rangle = 4\pi\frac{1}{L^3}\left\langle|F|^2\right\rangle$$

$$= \frac{k_0^4}{\pi}P(k_0\mathbf{e}_r - k_0\mathbf{e}_3) = \frac{k_0^4}{\pi}P\left(2k_0\sin\frac{\psi}{2}\right)$$

Ray bending parameter

$$g_0(\omega) = \frac{1}{4\pi}\oint g(\psi,\omega)d\Omega$$

g_0^{-1} : Mean free path

Exponential ACF:

$$g(\psi;\omega) = \frac{8\varepsilon^2 a^3 k_0^4}{\left(1+4a^2k_0^2\sin^2\frac{\psi}{2}\right)^2}$$

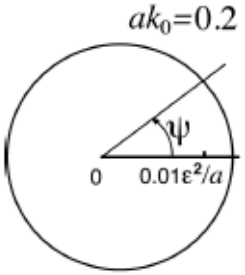

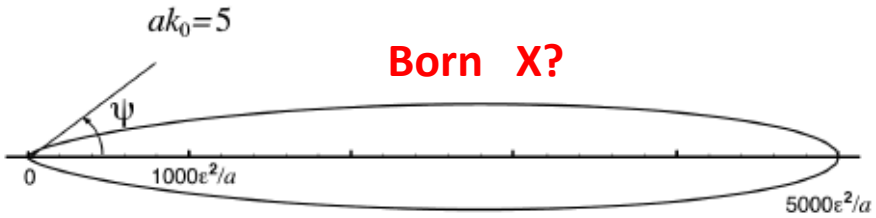

Born X?

Radiative Transfer Equation (Boltzmann equation) in Scattering Media

$$\partial_t f(\mathbf{x},t;\mathbf{q}) + V_0\mathbf{q}\nabla f(\mathbf{x},t;\mathbf{q}) = -g_0(k_0)V_0 f(\mathbf{x},t;\mathbf{q}) + \frac{V_0}{4\pi}\oint g(k_0\mathbf{q}-k_0\mathbf{q}')f(\mathbf{x},t;\mathbf{q}')\,d\Omega_{q'} + W(\omega)\frac{\Psi(\mathbf{q})}{4\pi}\delta(\mathbf{x})\delta(t)$$

$$E(\mathbf{x},t) = \oint f(\mathbf{x},t,\mathbf{q})d\Omega_q$$

Ray bending

$$g(k_0\mathbf{q}) = \frac{k_0^4}{\pi}P(k_0\mathbf{q})$$

$$k_0 = \frac{\omega}{V_0}$$

$$g_0(k_0) = \frac{1}{4\pi}\oint g(k_0\mathbf{q})d\Omega_q \qquad \oint \Psi(\mathbf{q})d\Omega_{\mathbf{q}} = 4\pi$$

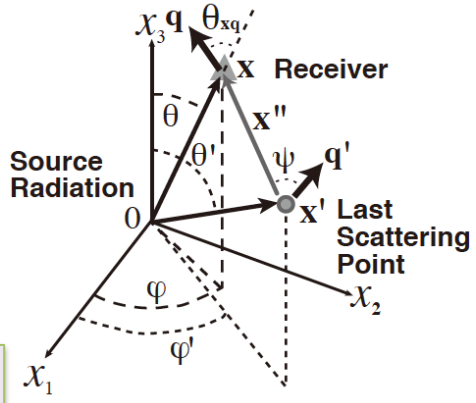

f(**x**,t,**q**): Directional distribution of energy density to direction ***q*** (Specific intensity)
E (**x**,t): Energy density in a band having center at ω_0
V_0: Propagation velocity
P(**m**): Power spectral density of velocity fractional fluctuation
$g(k_0\mathbf{q})$: Scattering coefficient at wavenumber k_0 to direction ***q***
$g_0(k_0)$: Total scattering coefficient at wavenumber k_0
W: Total radiated energy
$\Psi(\mathbf{q})$: Radiation pattern

Phenomenological equation satisfying energy conservation.

Diffusion Approximation

At a large lapse time, we may expect that spatial distribution of f is smooth.
Boltzmann eq. is well approximated by the diffusion equation:

$$\partial_t E - D\Delta E = W\delta(\mathbf{x})\delta(t)$$

$$D = V_0/(3g_m)$$

Transport Scattering Coefficient (TrSC):

$$g_m(\omega_0) = \frac{1}{4\pi}\oint g(k_0,\psi)(1-\cos\psi)d\Omega$$
$$= \frac{1}{4\pi}\int_0^{2k_0} P(m)m^3 dm.$$

Total Scattering Coefficient :

$$g_0(\omega_0) = \frac{1}{4\pi}\oint g(k_0,\psi)d\Omega$$
$$= \frac{k_0^2}{2\pi}\int_0^{2k_0} P(m)m dm$$

$g_m(k_0)$ works as an effective isotropic scattering coefficient even if $g(k_0\mathbf{q})$ is nonisotropic.

$$E(\mathbf{x},t) = \frac{W}{(4\pi Dt)^{3/2}} e^{-\frac{r^2}{4Dt}} H(t)$$

Radiative Transfer Equation in Integral Form

$$f(\mathbf{x},t;\mathbf{q}) = W\Psi(\mathbf{q})\,G_R(\mathbf{x},t;\mathbf{q}) + V_0\int_{-\infty}^{\infty}dt'\iiint_{-\infty}^{\infty}d\mathbf{x}'G_R(\mathbf{x}-\mathbf{x}',t-t';\mathbf{q})\oint g(k_0\mathbf{q}-k_0\mathbf{q}')\,f(\mathbf{x}',t';\mathbf{q}')\,d\Omega_{q'}.$$

Propagator: $G_R(\mathbf{x},t;\mathbf{q}) = \delta_\Omega(\mathbf{x};\mathbf{q})\,G(\mathbf{x},t)$

$$G(\mathbf{x},t) = \delta\left(t-\frac{|\mathbf{x}|}{V_0}\right)\frac{e^{-g_0V_0t}}{4\pi V_0|\mathbf{x}|^2}H(t)$$

Causality, Geometrical decay factor, Scattering loss

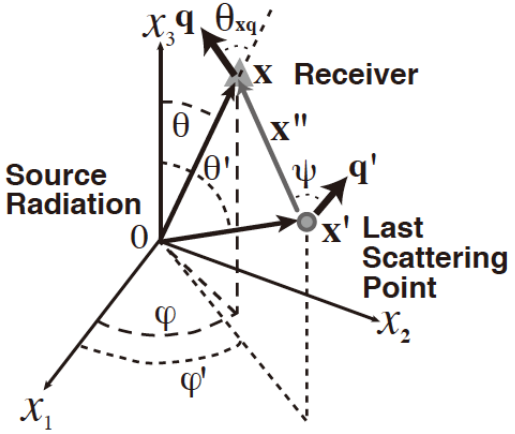

$\delta_\Omega(\mathbf{x};\mathbf{q})$: Delta function in solid angle
Propagation is on the ray direction

Multiple isotropic scattering model for coda excitation

$g_0 = g_m$

Spherical source radiation and isotropic scattering:

$$E(\mathbf{x},t) = W\,G(\mathbf{x},t) + V_0 g_0 \int_{-\infty}^{\infty} G(\mathbf{x}-\mathbf{x}',t-t')E(\mathbf{x}',t')\,d\mathbf{x}'dt'$$

$$G(\mathbf{x},t) = \frac{1}{4\pi r^2 V_0}\delta\left(t-\frac{r}{V_0}\right)e^{-g_0 V_0 t} \qquad \Rightarrow \frac{1}{4\pi r^2 V_0}\delta\left(t-\frac{r}{V_0}\right)e^{-g_0 V_0 t - Q_I^{-1}\omega_0 t}$$

Q_I^{-1} : Intrinsic absorption at ω_0

Fourier transform:

$$E(\mathbf{x},t) = \frac{1}{(2\pi)^4}\iiint\int_{-\infty}^{\infty}\hat{\tilde{E}}(\mathbf{k},\omega)e^{i(\mathbf{kx}-\omega t)}d\mathbf{k}d\omega$$

Radiative transfer equation in the Fourier space:

$$\hat{\tilde{E}}(\mathbf{k},\omega) = \frac{W\hat{\tilde{G}}(\mathbf{k},\omega)}{1-g_0 V_0\hat{\tilde{G}}(\mathbf{k},\omega)}$$

Series expansion [Born approximation]

$$\hat{\tilde{E}}(\mathbf{k},\omega) \approx W\hat{\tilde{G}}\left[1+g_0 V_0\hat{\tilde{G}}+\left(g_0 V_0\hat{\tilde{G}}\right)^2+\left(g_0 V_0\hat{\tilde{G}}\right)^3\cdots\right]$$

Temporal Change and Spatial Dist. of Energy Density

Isotropic Scattering Process for Spherical Source Radiation [Zeng et al. 1991]

To multiply Exp[$-Q_l^{-1}\,\omega_0 t$] in the presence of intrinsic absorption

$$\bar{t} = g_0 V_0 t, \quad \bar{r} = g_0 r$$

$$\bar{E} = \frac{E}{W g_0^3}$$

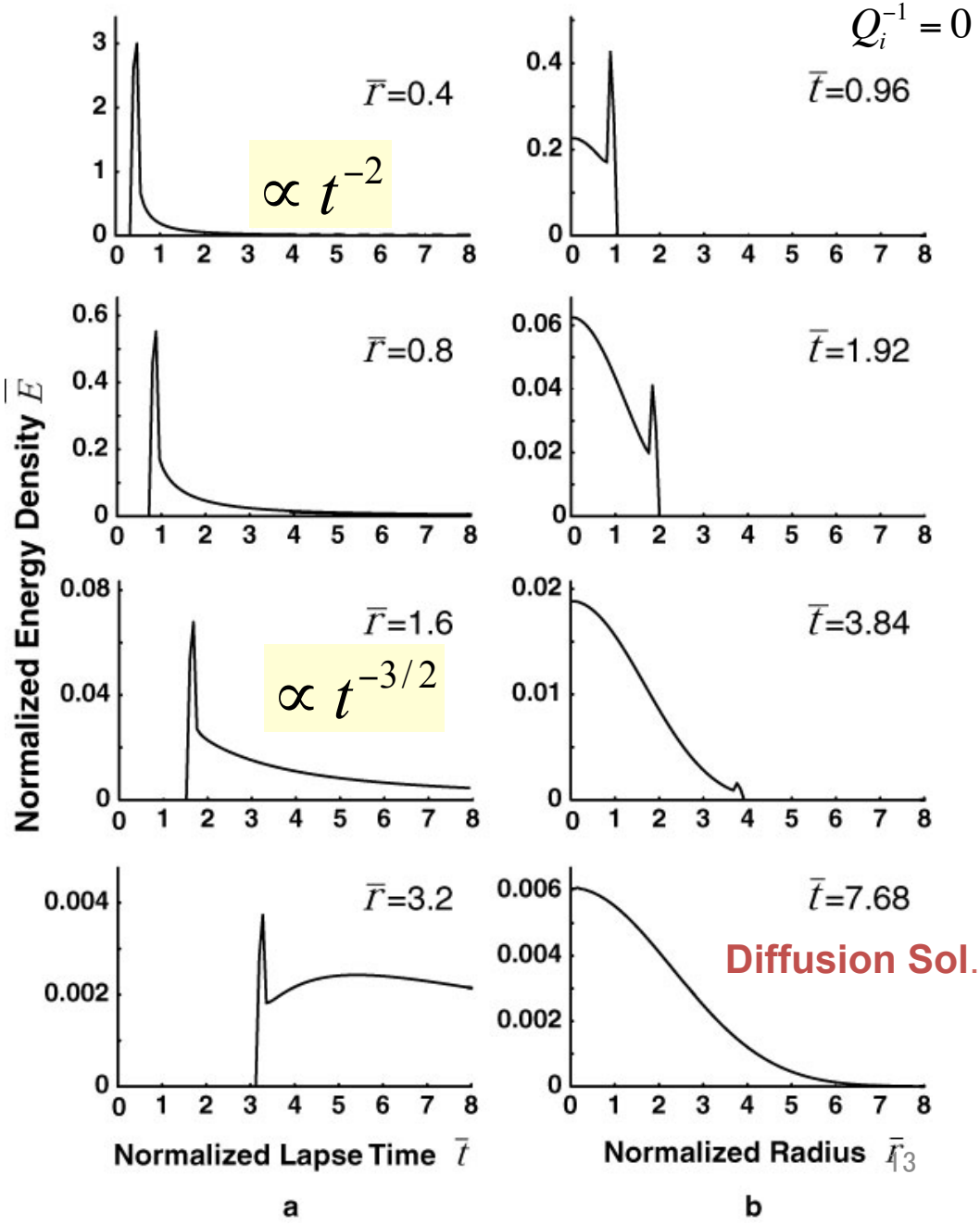

Multiple Lapse Time Window Analysis [Fehler et al. 1991]

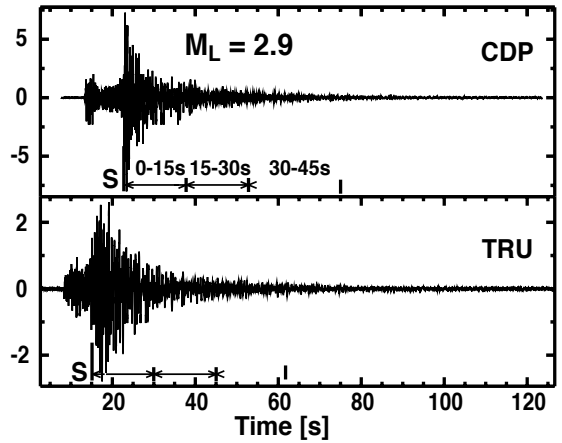

To plot the logarithm of the energy obtained from each window as a function of the hypocentral distance.

To perform a non-linear fit by using a simple model (isotropic scattering and intrinsic absorption): $Q_S^{-1} = V_0 g_0 / \omega$ and Q_i^{-1}

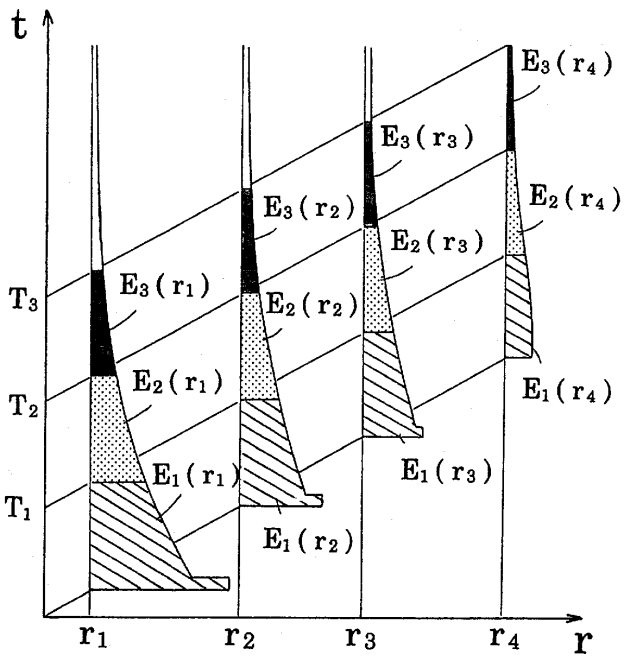

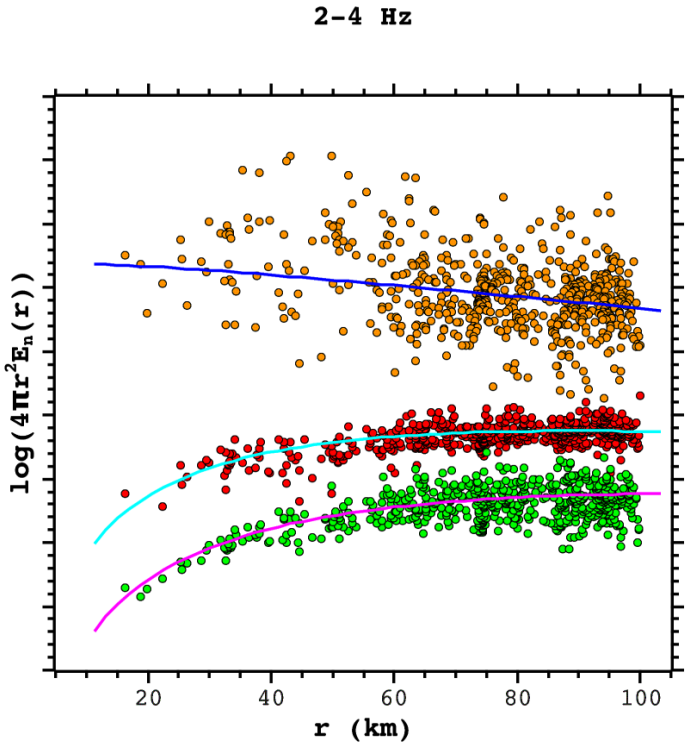

Scattering Loss
(Spatial smoothing)

$$Q_S^{-1} = V_0 g_0 / \omega$$

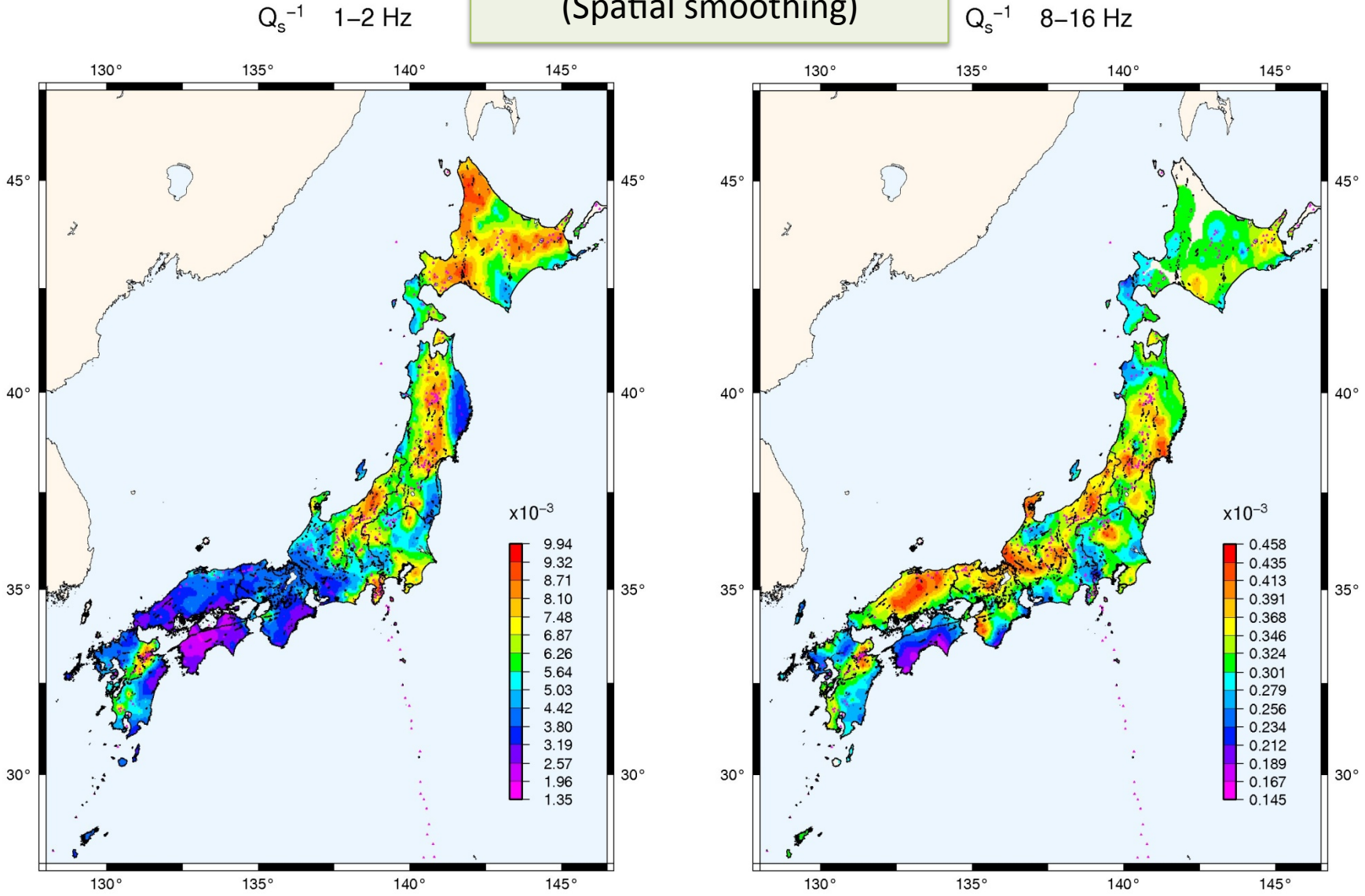

Hi-net: 772 stations,
135,000 events (D<40km)

Carcole and Sato [2010]

Intrinsic Absorption (Spatial smoothing)

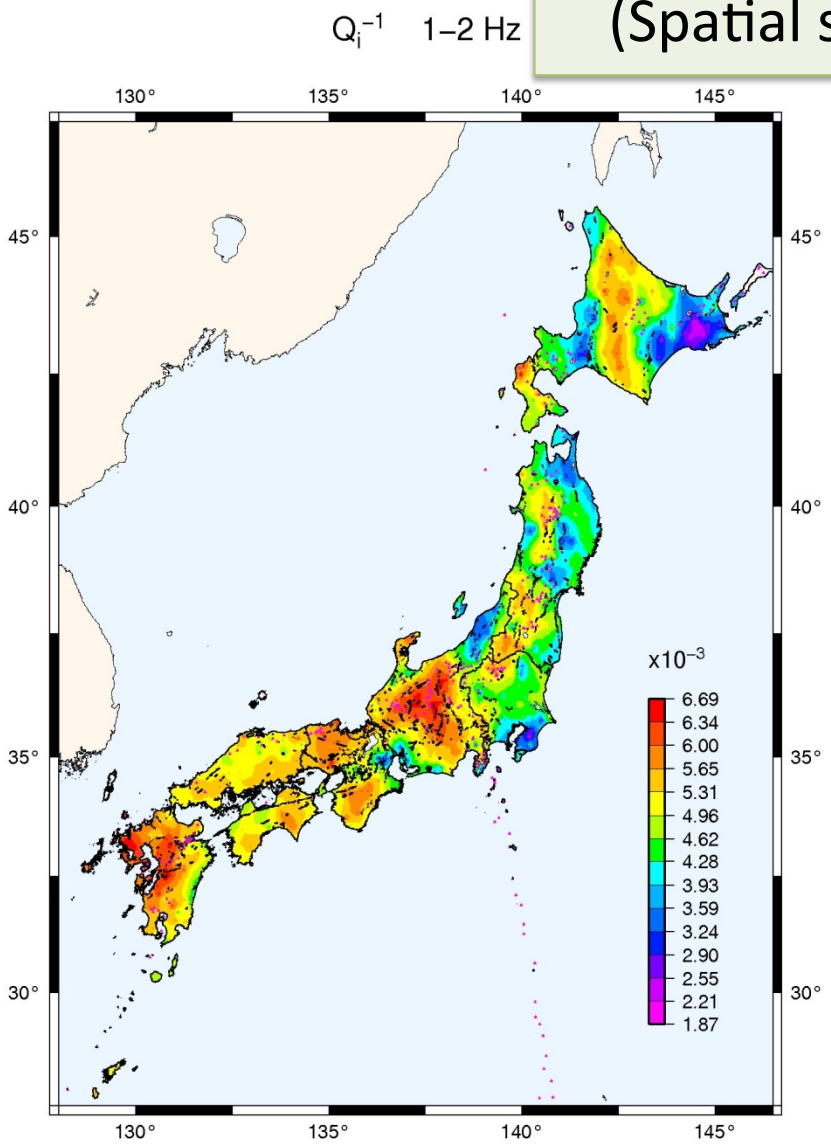

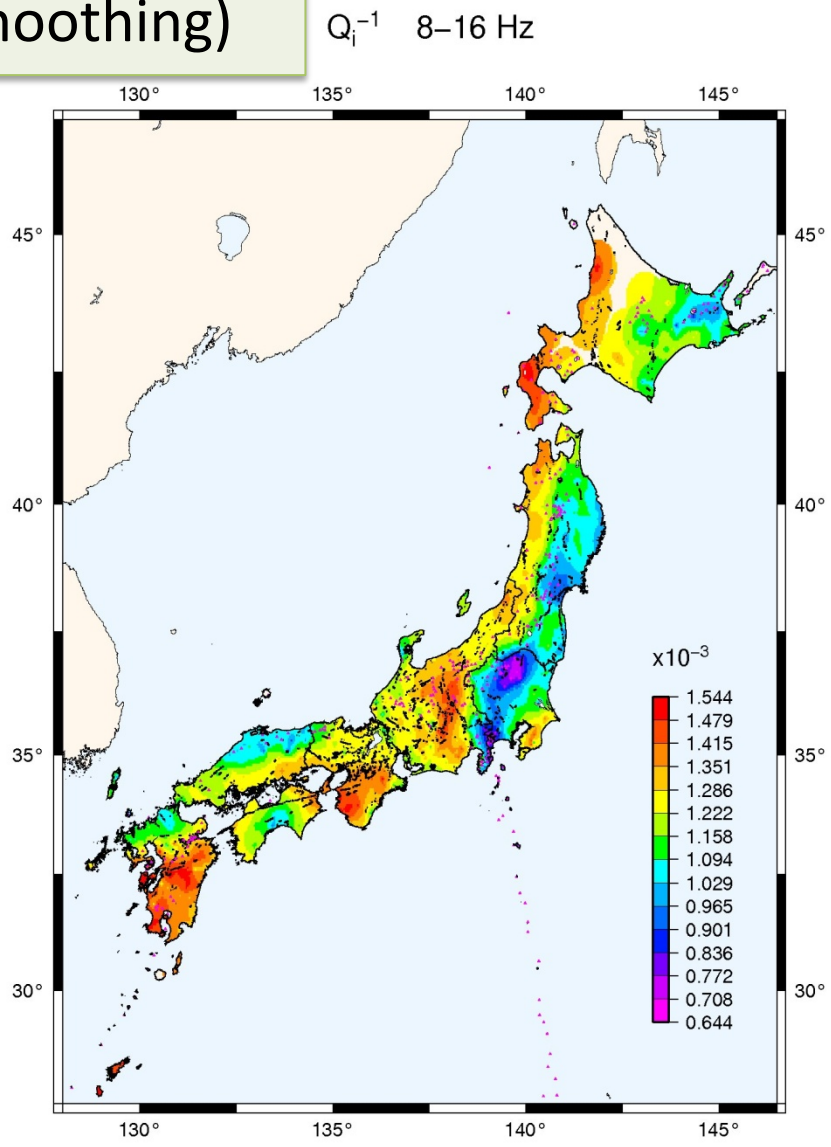

Carcole and Sato [2010]

Multiple Isotropic Scattering Model with PS Conversion

Two velocity modes

$$E(\boldsymbol{x},t) = E^P(\boldsymbol{x},t) + E^S(\boldsymbol{x},t)$$

$$E^P(\boldsymbol{x},t) = W^P G^P(\boldsymbol{x},t) + \iiiint \left\{E^P(\boldsymbol{x}',t')\alpha_0 g_0^{PP} + E^S(\boldsymbol{x}',t')\beta_0 g_0^{SP}\right\} G^P(\boldsymbol{x}-\boldsymbol{x}',t-t')dt'dx'$$

$$E^S(\boldsymbol{x},t) = W^S G^S(\boldsymbol{x},t) + \iiiint \left\{E^S(\boldsymbol{x}',t')\beta_0 g_0^{SS} + E^P(\boldsymbol{x}',t')\alpha_0 g_0^{PS}\right\} G^S(\boldsymbol{x}-\boldsymbol{x}',t-t')dt'dx'$$

$$G^P(\boldsymbol{x},t) = \frac{1}{4\pi r^2 \alpha_0} H(t)\,\delta\left(t-\frac{r}{\alpha_0}\right)\exp\left(-(\alpha_0 g_0^{PP} + \alpha_0 g_0^{PS} + b)t\right)$$

$$G^S(\boldsymbol{x},t) = \frac{1}{4\pi r^2 \beta_0} H(t)\,\delta\left(t-\frac{r}{\beta_0}\right)\exp\left(-(\beta_0 g_0^{SS} + \beta_0 g_0^{SP} + b)t\right)$$

g : Total scattering coefficient**

Intrinsic attenuation $b = \omega Q_i^{-1}$

Sato [1994]

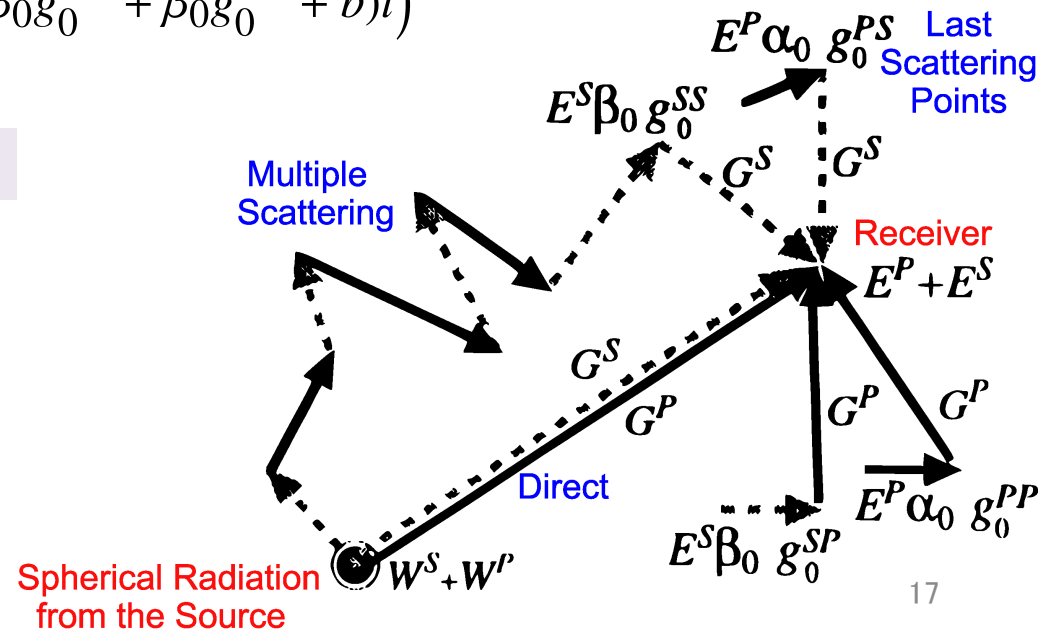

Structure Study Experiment of Asama Volcano, Japan in 2006

5 Shots, 250-350 kg TNT at 60m in depth.

464 stations (2Hz velocity seismometers) with a 100m separation

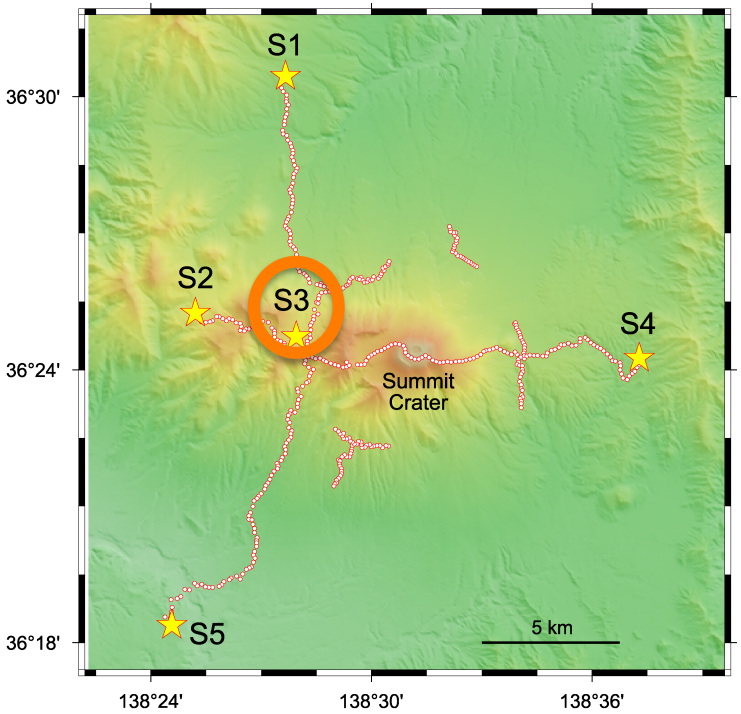

Explosion…P-Source

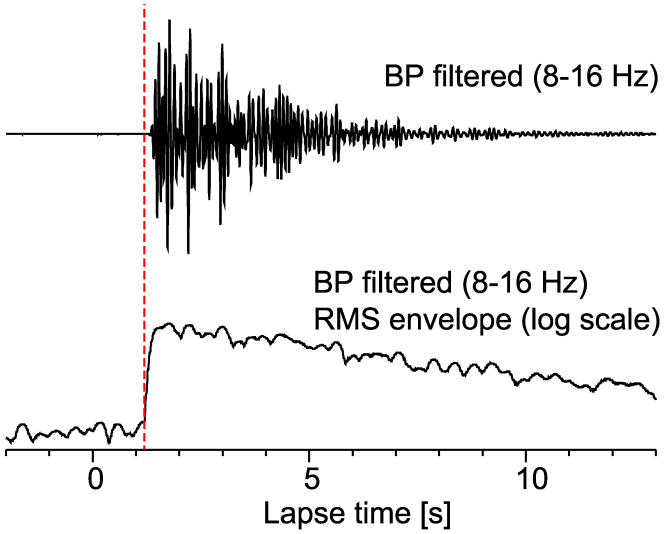

Temporal Change in the Spatial Distribution of Seismic Energy Density (MS Amplitude)

- P-wave source (Explosion)
- Existence of wave front
- Energy concentration near the source
- Characterized by two different gradient lines
- Corner propagates with the S wave velocity

Band-pass filtering 8-16Hz
Coda normalization at 50s

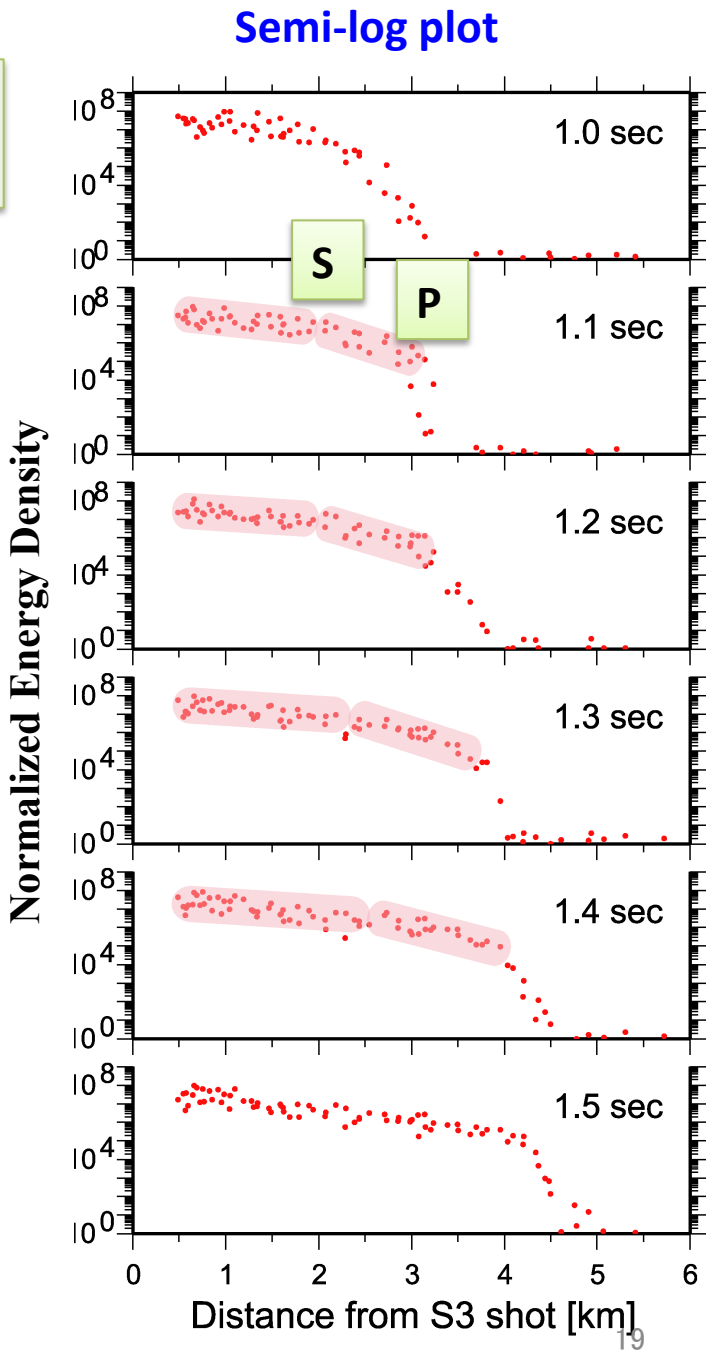

Estimation of total scattering coefficients

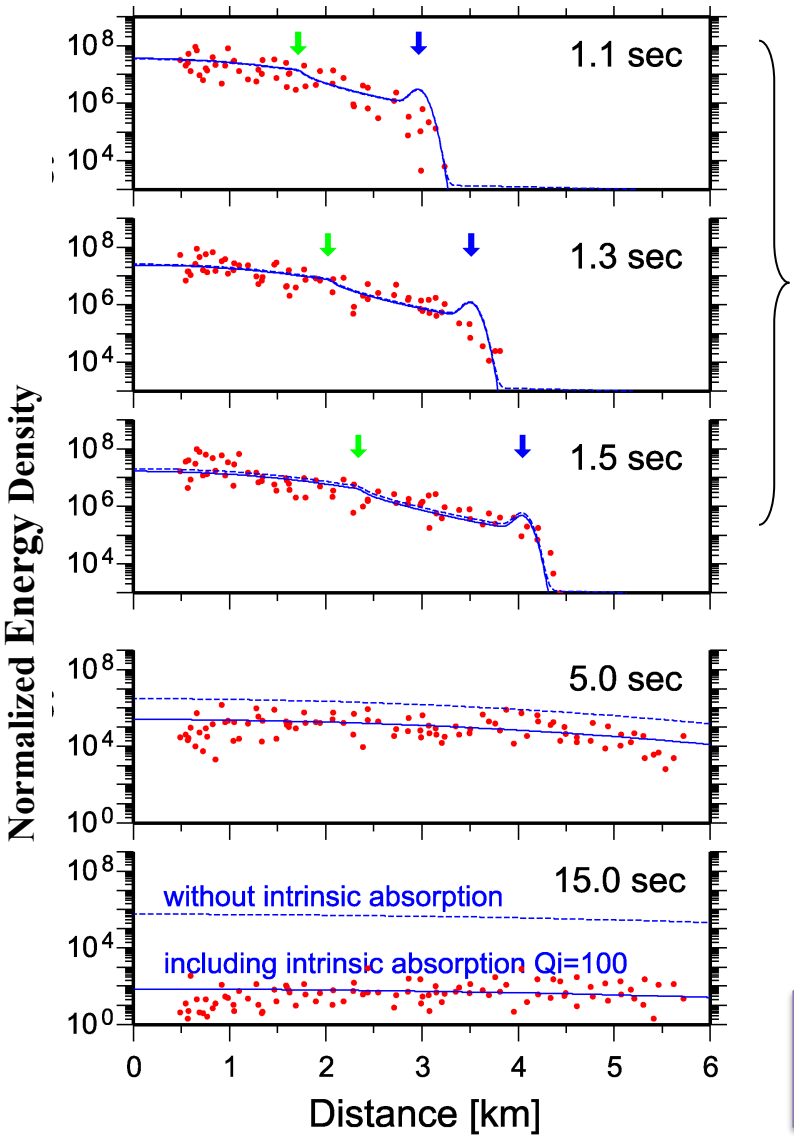

Assumption:
- **P wave source (Ws=0)**
- **3-D infinite medium (neglect surface effect)**

Parameters:
- **Initial P wave energy W_P**
- **P wave velocity**
- **Isotropic scattering coefficients (g^{pp}, g^{ps}, g^{ss}),**

Constraint: $\frac{\alpha_0}{\beta_0} = \sqrt{3}, \quad \frac{g_0^{PS}}{g_0^{SP}} = 2\frac{\alpha_0^2}{\beta_0^2} = 6$

By using grid search
Data at lapse time 1.0-1.5s

$$\alpha_0 = 2.7\,\mathrm{km/s},\ \beta_0 = 1.56\,\mathrm{km/s}$$
$$g_0^{PP} = 0.26\mathrm{km}^{-1},\ g_0^{PS} = 0.63\mathrm{km}^{-1}$$
$$g_0^{SP} = 0.11\mathrm{km}^{-1},\ g_0^{SS} = 0.79\mathrm{km}^{-1}$$

The estimated Q_i^{-1} =0.01 may contain intrinsic absorption and window effect.

Yamamoto and Sato [2010]

Total Scattering Coefficient in the Lithosphere

$g_0[\mathrm{km}^{-1}]$

g_m ?

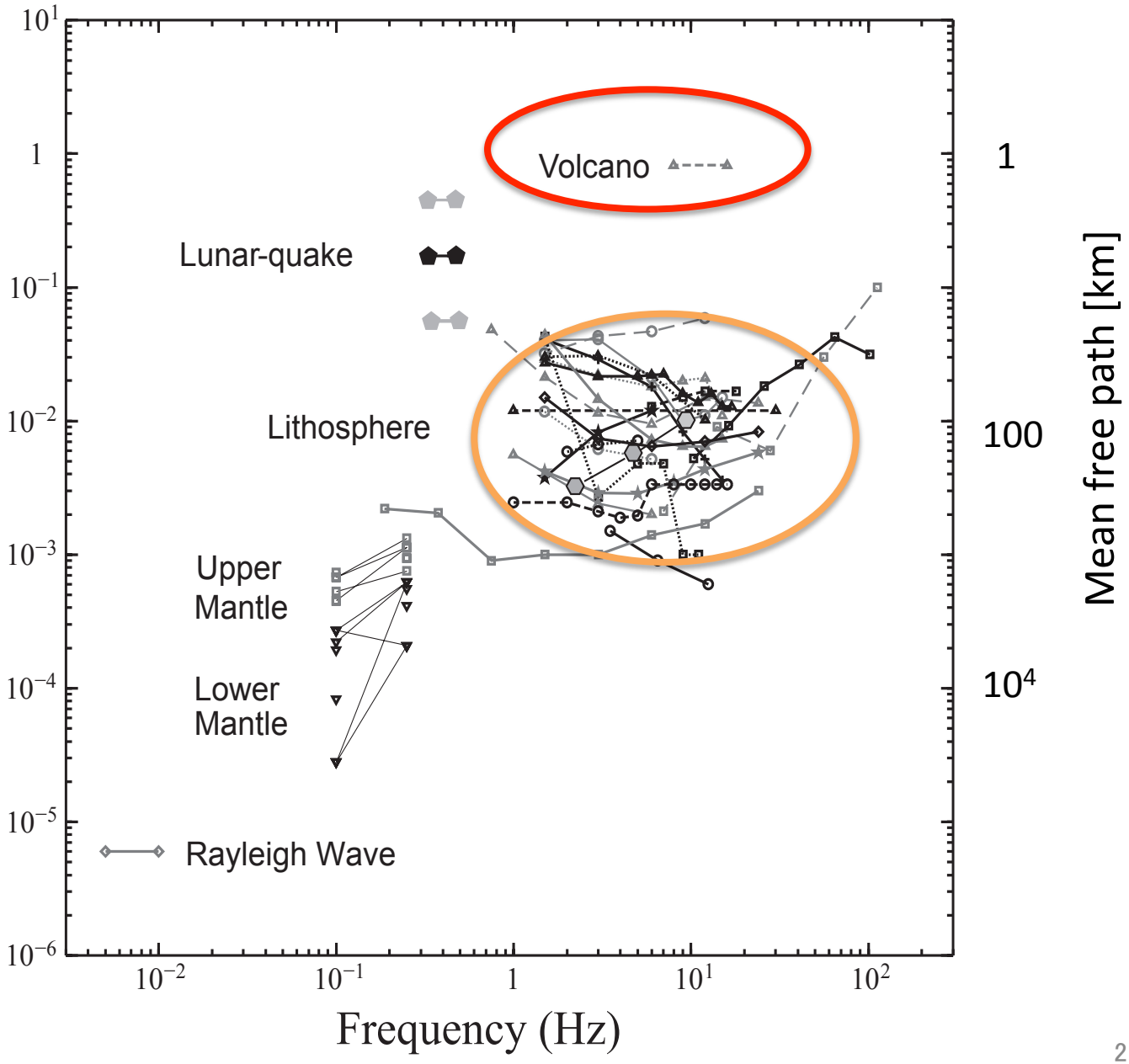

Frequency Dependence of Attenuation and Scattering in Japan

Intrinsic Absorption

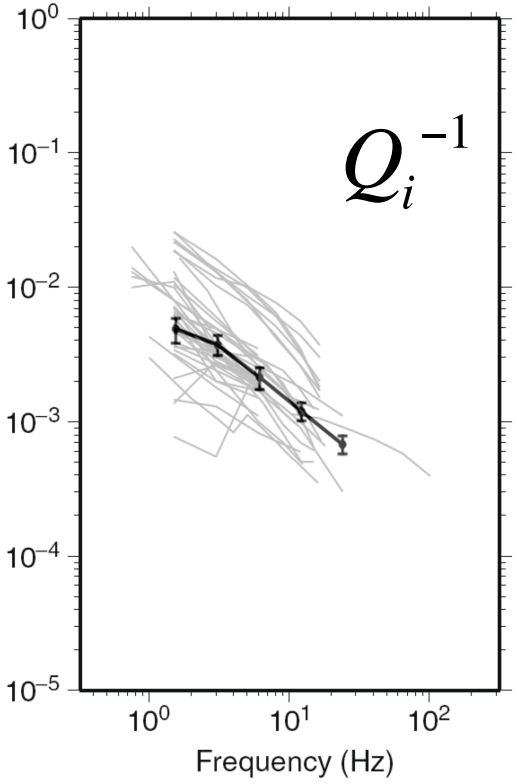

Scattering Loss

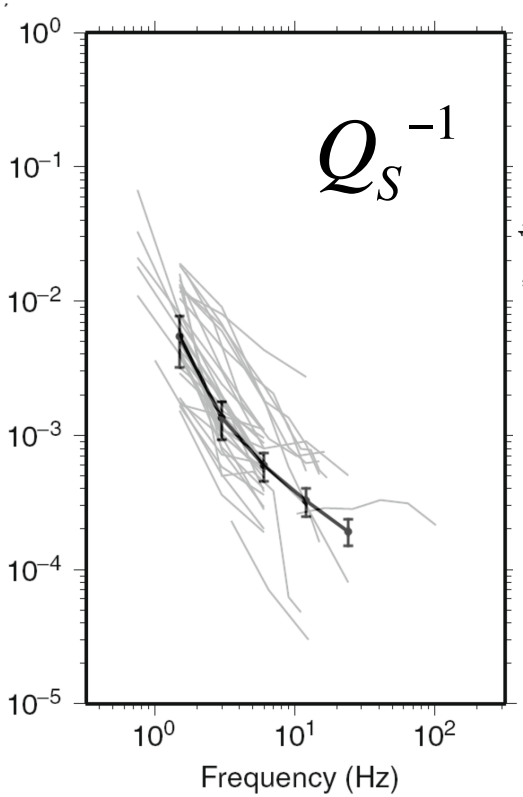

Scattering Coefficient

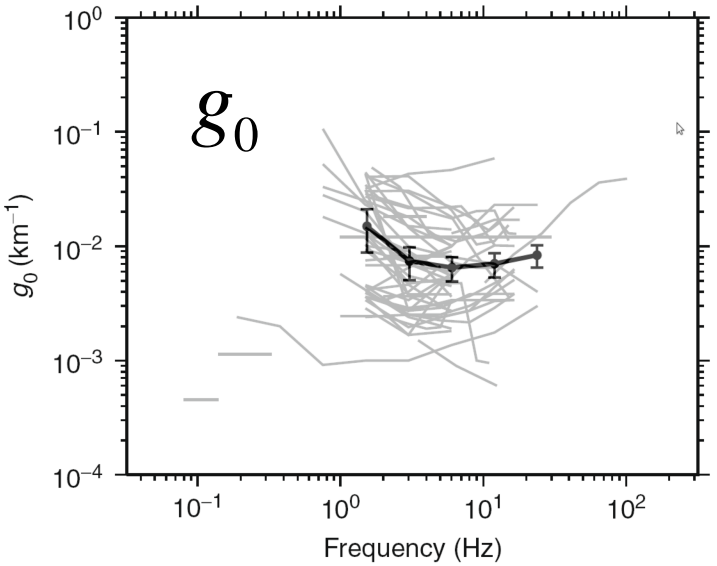

Carcole and Sato [2010]

$$E = W\Psi G + V_0 g_0 G * E$$

$$G(\mathbf{x},t) = \frac{1}{4\pi V_0 r^2} H(t)\delta\left(t - \frac{r}{V_0}\right) e^{-(V_0 g_0 + b)t}$$

$$\oint d\Omega\Psi(\theta,\phi) = 4\pi$$

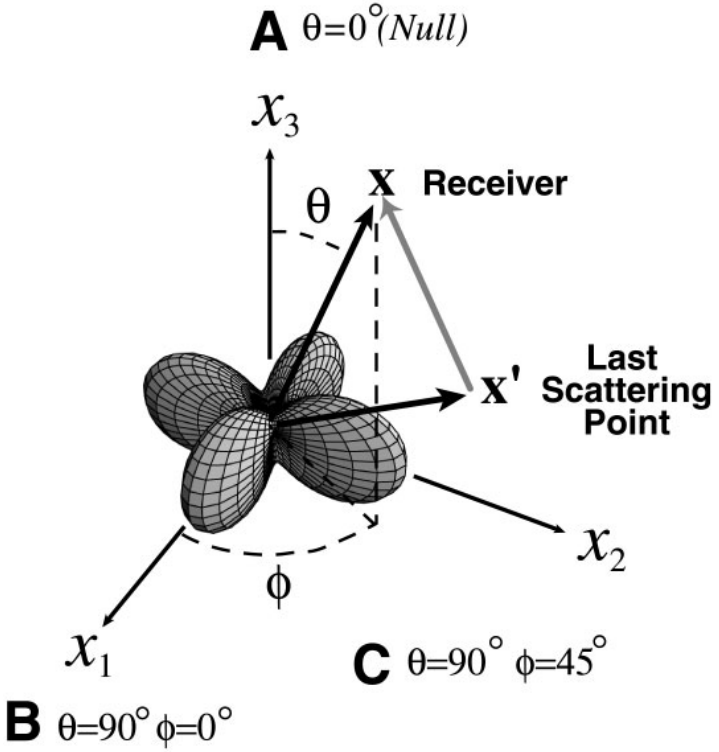

Point Shear Dislocation Source

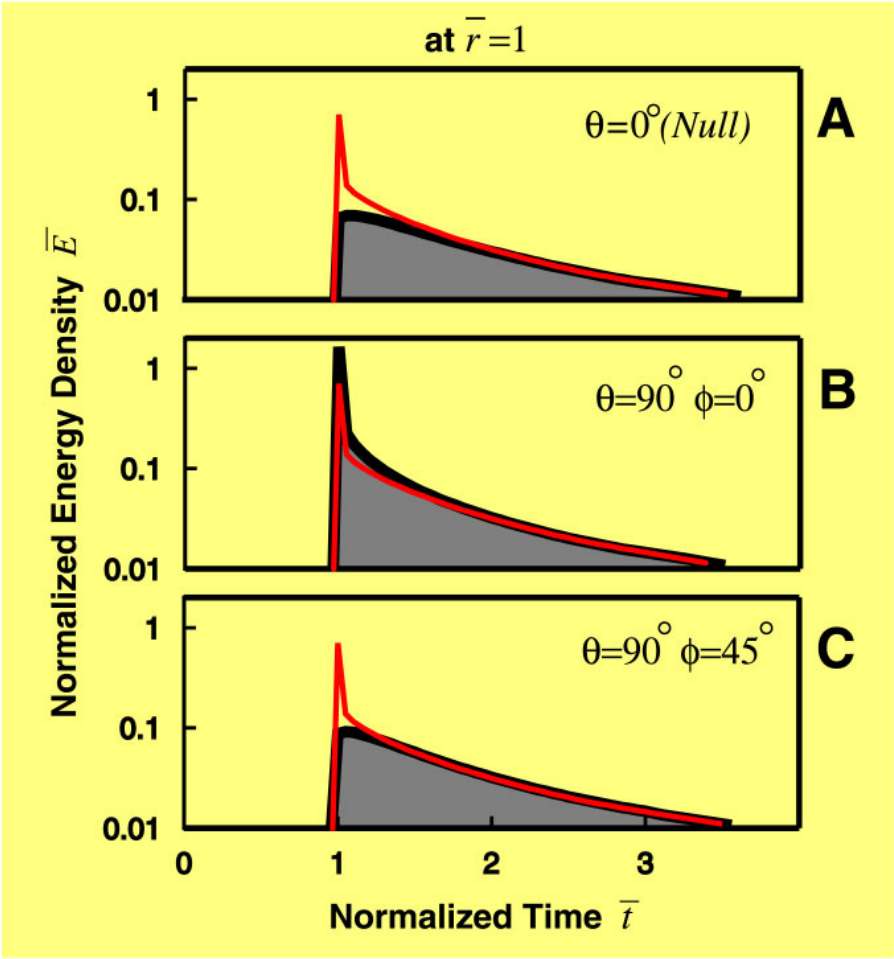

$$\bar{r} = g_0 r \text{ and } \bar{t} = g_0 V_0 t$$ Sato et al. [1997]

Seismogram Envelope Inversion for the High Frequency Energy Radiation Hisotry

Deconvolution of observed S-wave envelopes by using the envelope Green function

E_{ij} : Energy Density (MS Amp.) at the i-th Station at the j-th Time

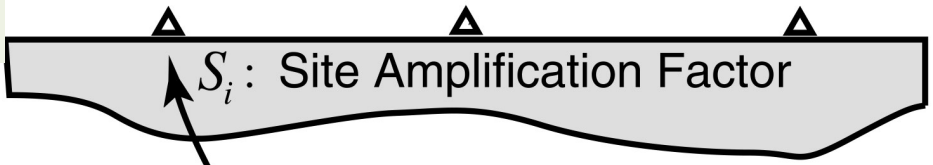

F_{ijk} : Envelope Green Function for a Point-Shear Dislocation Source

W_k : Radiated Energy from the k- th Subfault

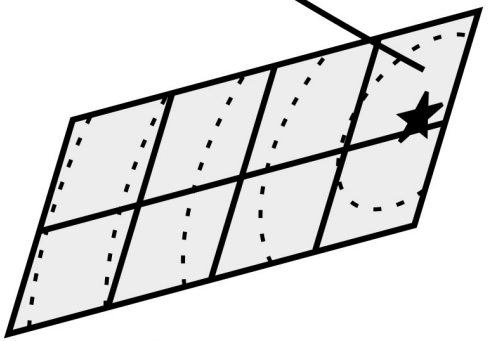

$$E_{ij} = S_i \sum_k F_{ijk} W_k$$

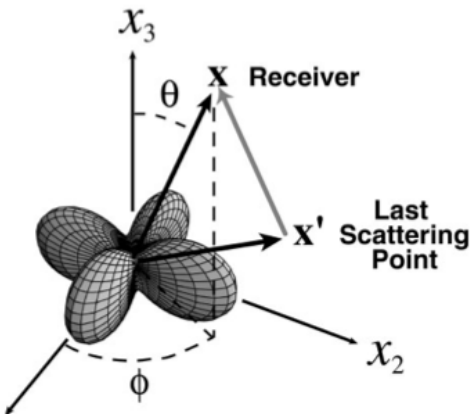

Point-shear dislocation source

$$\sum_{i,j} \frac{1}{\sigma_i^2} \left| E_{ij} - S_i^{(n-1)} \sum_k F_{ijk} W_k^{(n)} \right|^2 \Rightarrow \text{Min}$$

Positive constraint for W_k

where $\sigma_i = E_{ij}\big|_{\text{Max}}$

1994 Far-East off-Sanriku Earthquake (Mw 7.7)

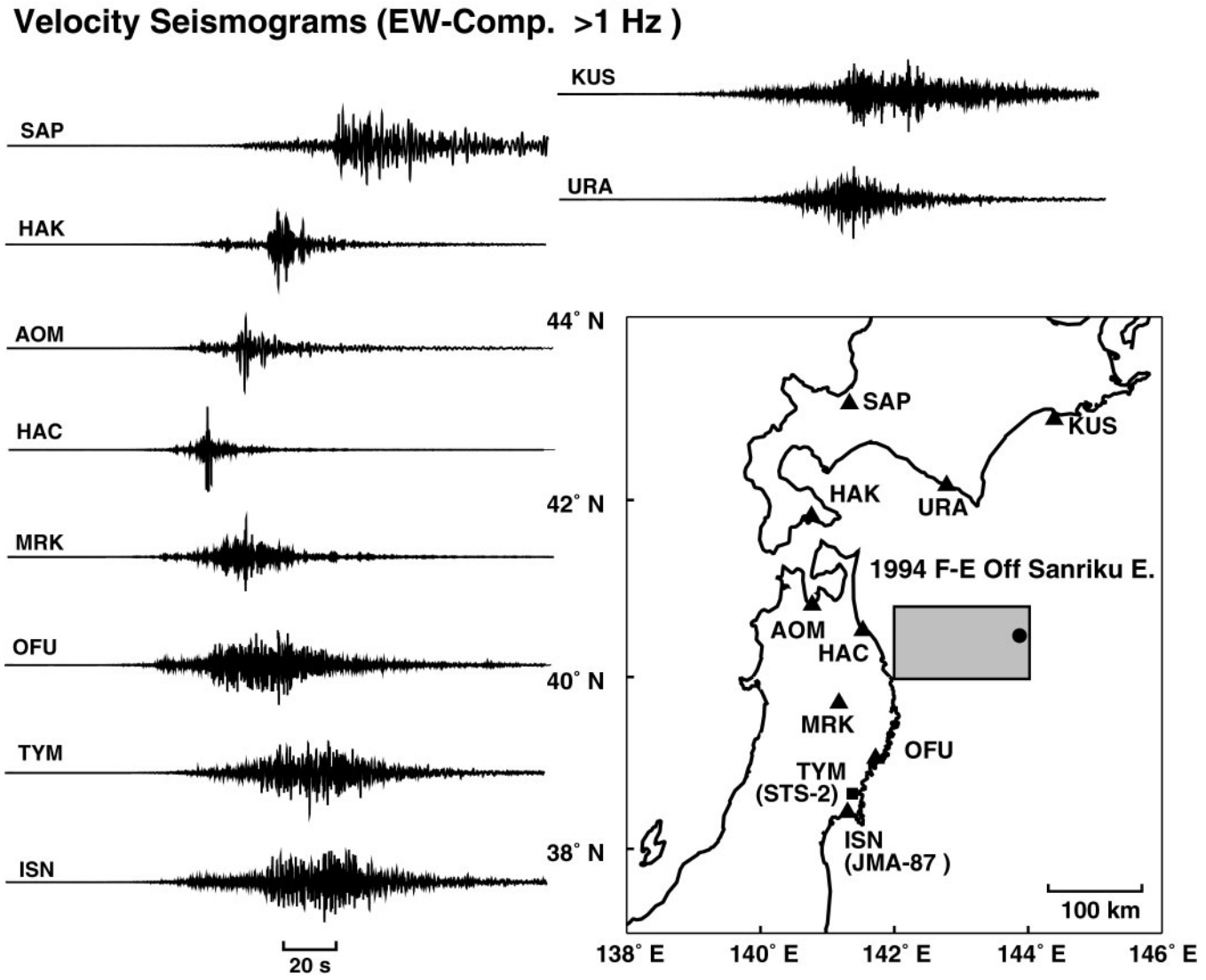

Nakahara et al. [1998]

Envelope Inversion Results

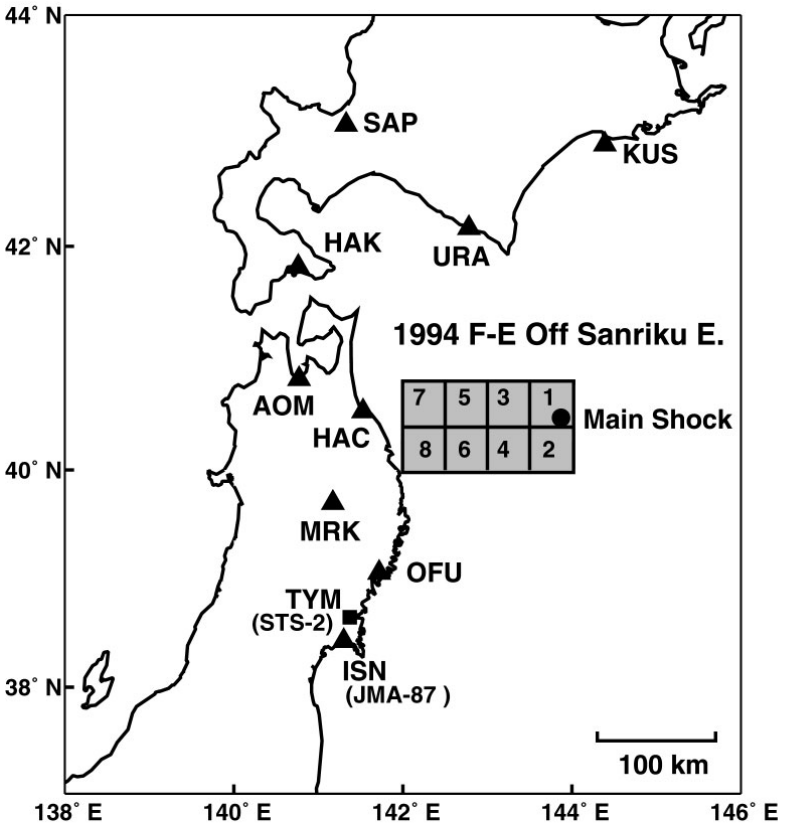

Strike 184°, Rake 70°
Dip 0° (E) ~ 30° (W)
After Harvard CMT
Vrup=2.7 km/s

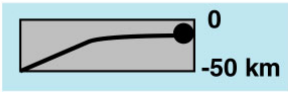

Vs=3.9 km/s, g_0=0.005 km^{-1} for 1-16 Hz
Qi=400 (1-2 Hz) ~ 1500 (8-16 Hz)
After Hoshiba[1993] and Sakurai et al. [1995]

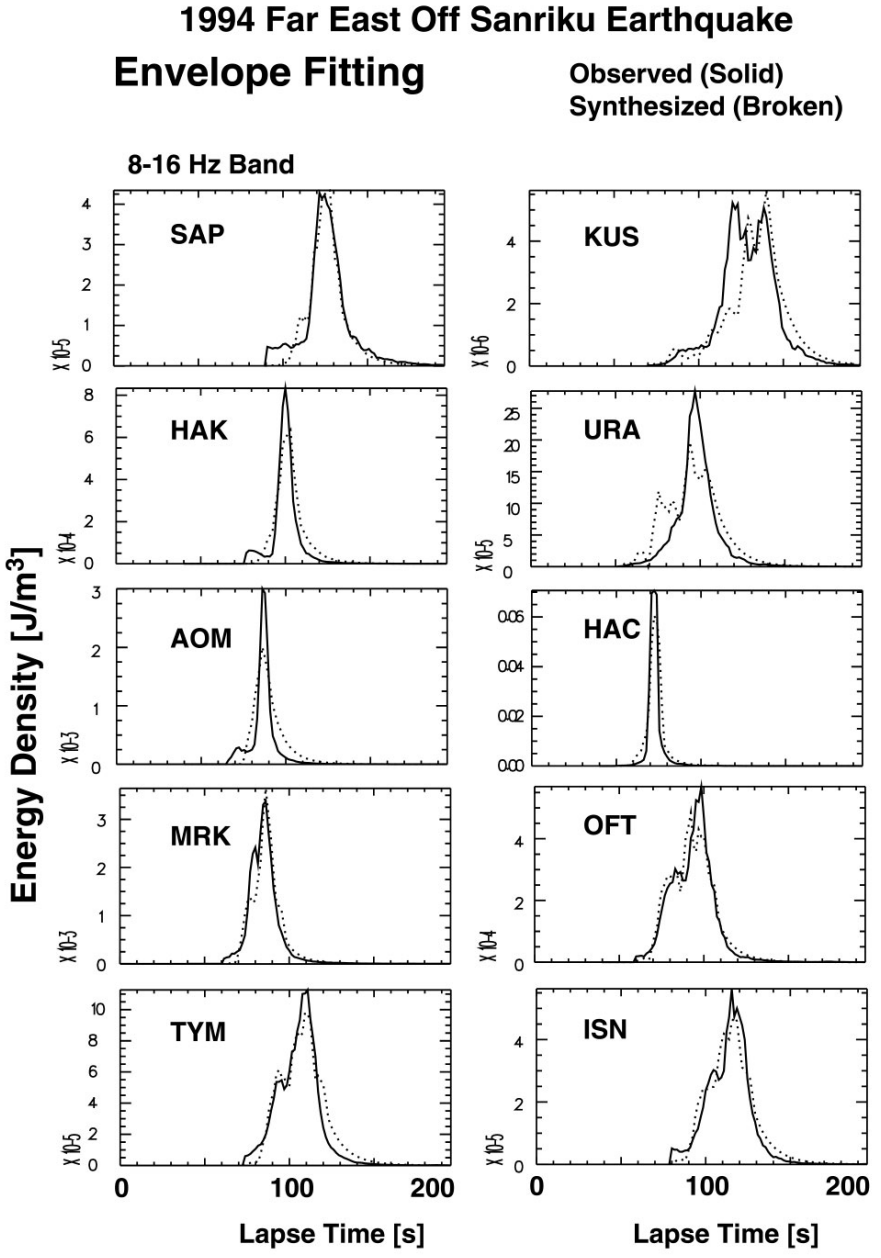

Nakahara et al. [1998]

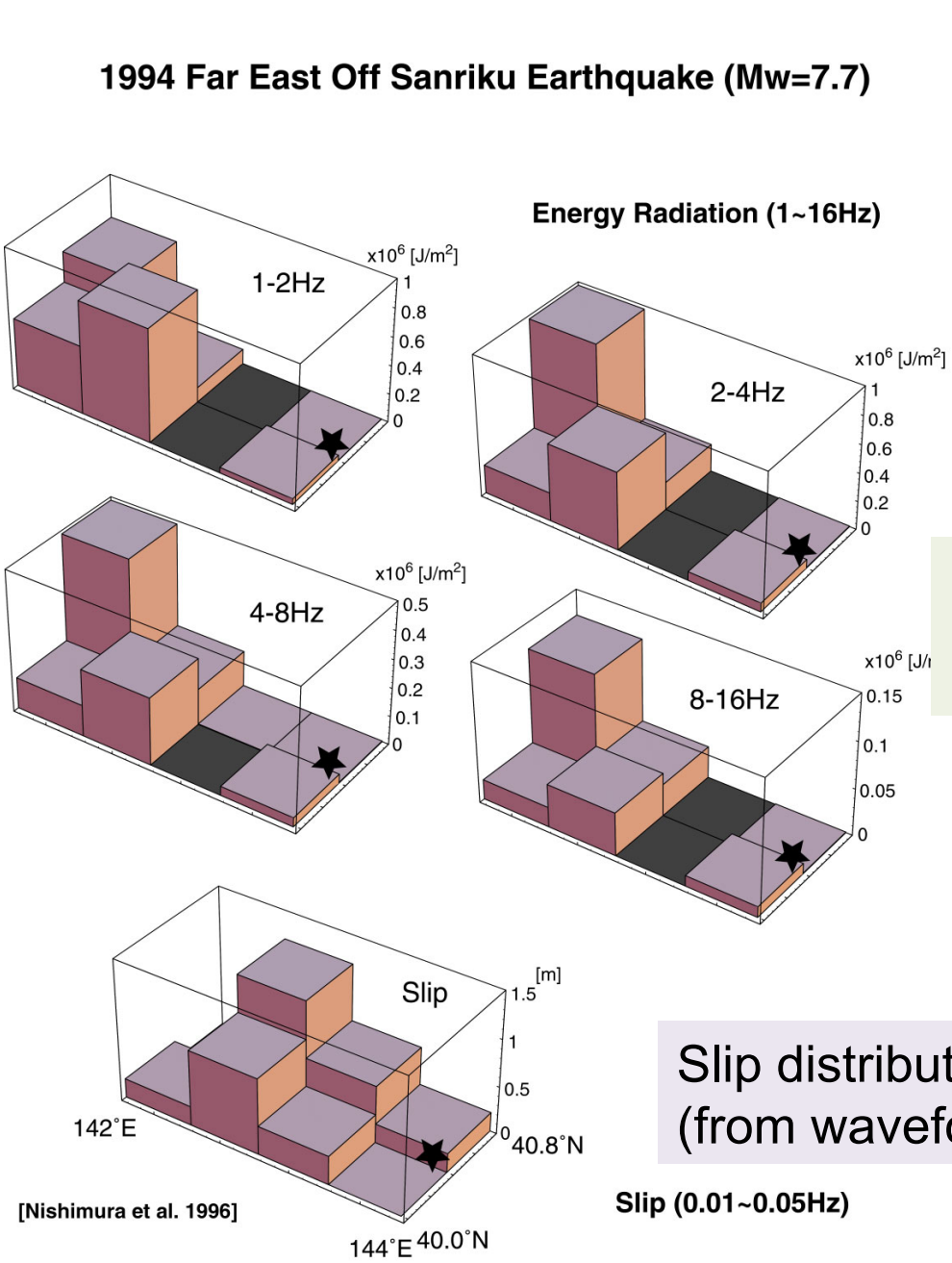

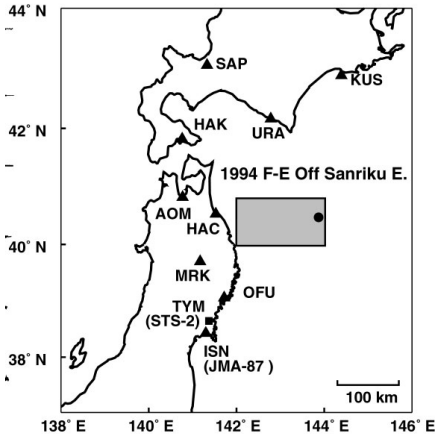

Radiation of high freq. energy
(from envelope inversion)

Slip distribution
(from waveform inversion)

[Nakahara et al. 1998]

Envelope Broadening with Travel Distance Increasing

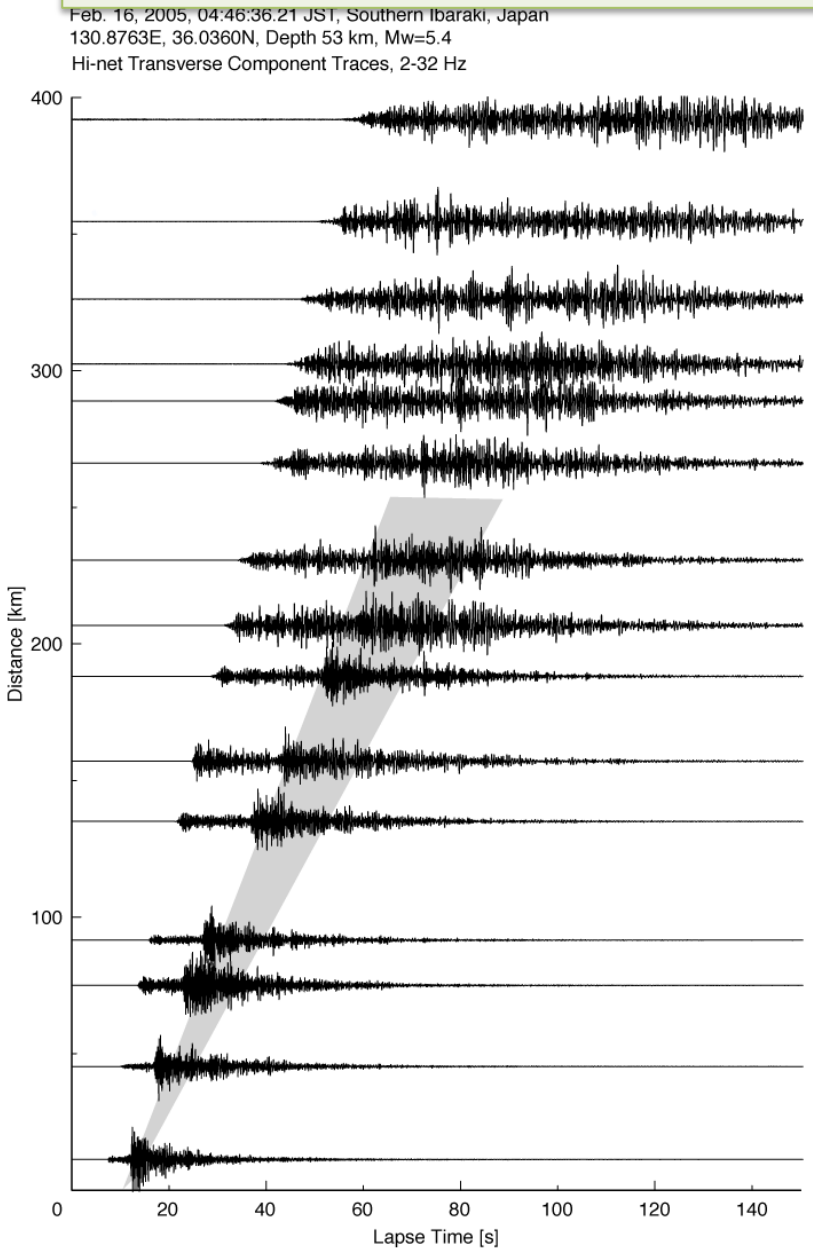

Focus on envelope width and peak delay from the S-onset

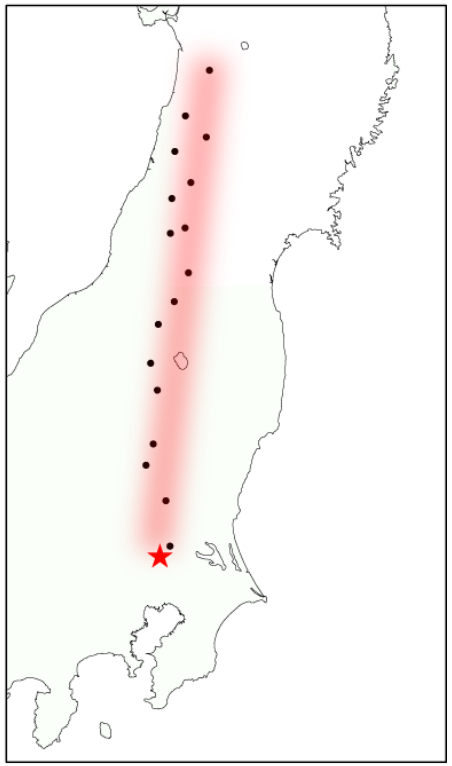

Courtesy of T. Maeda

Waves around the direct arrival are forward scattered waves (diffracted waves).

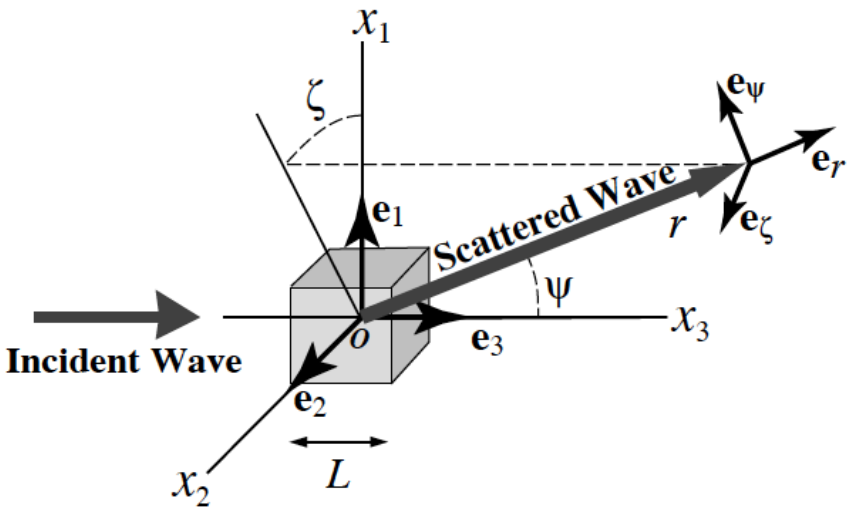

Strong forward scattering (diffraction) for λ << a

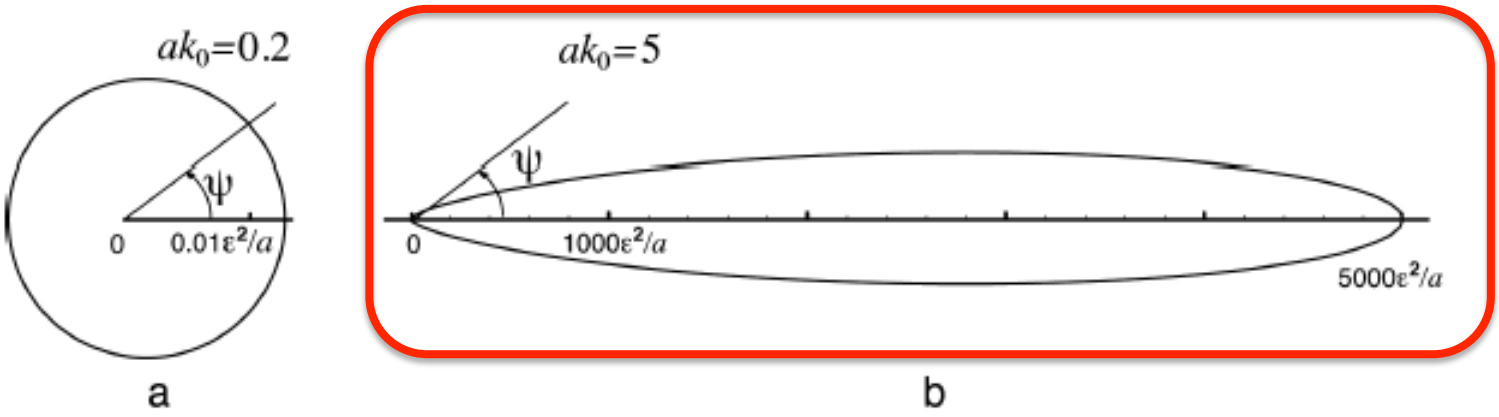

Fig. 4.3 Angular dependence of scattering coefficient (4.29) for scalar waves in 3-D random media characterized by an exponential ACF: (a) Low wavenumber case. (b) high wavenumber case.

Radiative Transfer Equation (Boltzmann equation) in Scattering Media

$$\partial_t f(\mathbf{x},t;\mathbf{q}) + V_0 \mathbf{q} \nabla f(\mathbf{x},t;\mathbf{q}) = -g_0(k_0) V_0 f(\mathbf{x},t;\mathbf{q}) + \frac{V_0}{4\pi} \oint g(k_0\mathbf{q} - k_0\mathbf{q}') f(\mathbf{x},t;\mathbf{q}') d\Omega_{q'} + W(\omega) \frac{\Psi(\mathbf{q})}{4\pi} \delta(\mathbf{x}) \delta(t)$$

$$E(\mathbf{x},t) = \oint f(\mathbf{x},t,\mathbf{q}) d\Omega_q \qquad g_0(k_0) = \frac{1}{4\pi} \oint g(k_0\mathbf{q}) d\Omega_q$$

Using the Fourier transform of *f* in space and time, and spherical harmonic expansion of *g* for scattering angle, we can write down the above equation as linear equations using Wigner 3-*j* symbols [Sato, 1995]

Inversion of scattering pattern from the envelope analysis of the 2008 Wells Earthquakes in Nevada, USA

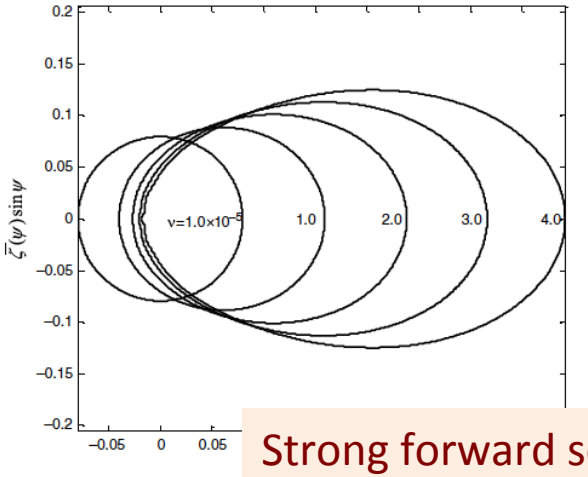

$$g(\psi) \propto \frac{1+\nu}{\left(1+\nu \sin^2 \frac{\psi}{2}\right)^2}$$

RMS envelope in 8-16 Hz (Event 4)

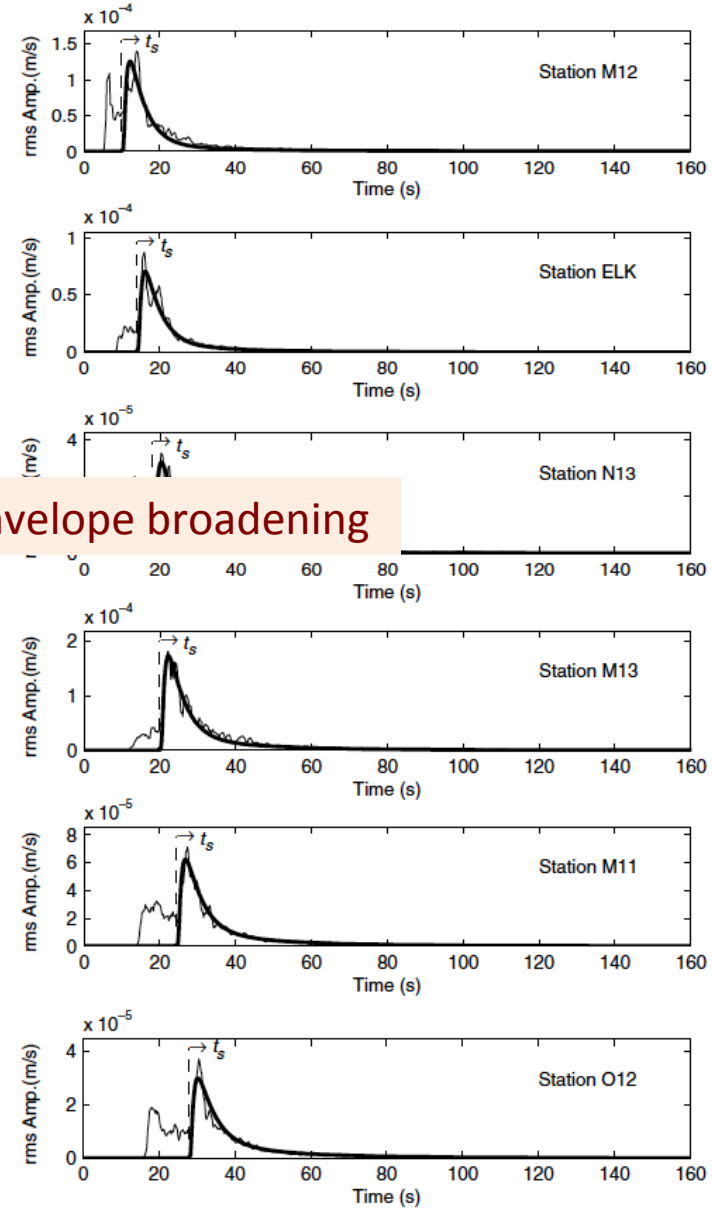

Strong forward scattering (diffraction)=Envelope broadening

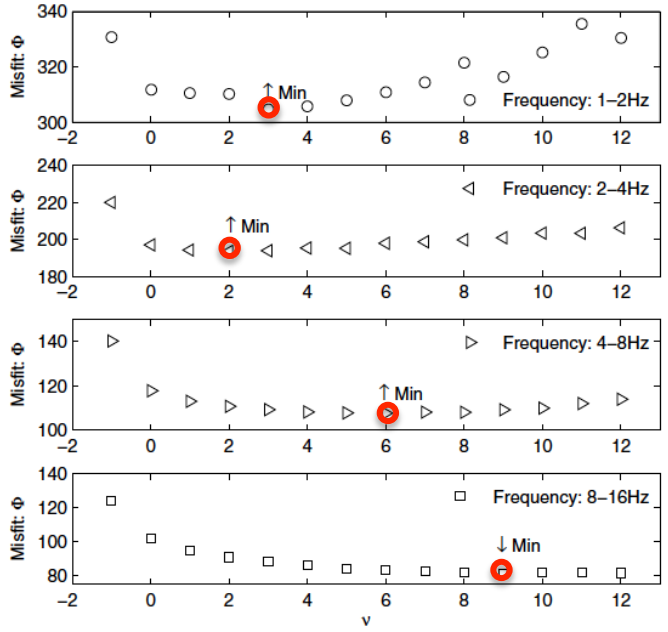

Figure 6. The change of misfit of event 4 with different scattering patterns. Arrows denote the minimum of misfits.

[Jing et al. 2014]

Markov approximation: stochastic extension of the phase screen method

Spherically outgoing wavelet: $$u(r,\theta,\varphi,\omega)=\frac{1}{2\pi r}\int_{-\infty}^{\infty}U(\mathbf{x}_\perp,r,\omega)e^{ik_0r-i\omega t}d\omega,$$

When $a\,k_c$ >>1, we may apply the parabolic approximation:

$$2ik_c\partial_r U+\Delta_\perp U-2k_c^2\xi U=0$$

We define the two-freq. mutual coherence func. (TFMCF) on the transverse plane:

$$\Gamma_2\left(\mathbf{x}_{\perp c},\mathbf{x}_{\perp d},r,\omega',\omega''\right)\equiv\left\langle U\left(\mathbf{x}'_\perp,r,\omega'\right)U\left(\mathbf{x}''_\perp,r,\omega''\right)^*\right\rangle$$

Its Fourier transform gives the intensity spectral density:

$$\widehat{I}(r,t;\omega_c)=\frac{1}{2\pi r^2}\int_{-\infty}^{\infty}d\omega_d\,e^{-\imath\omega_d(t-r/V_0)}\,\Gamma_2(\boldsymbol{x}_{\perp c},\boldsymbol{x}_{\perp d}=0,r,\omega_c,\omega_d)$$

Longitudinal integral of *R*: $$A(r_{\perp d})=2\int_0^{\infty}R(r_{\perp d},z)dz$$

Delta correlation

$$R(\mathbf{x})=A(\mathbf{x}_\perp)\delta(z)$$

To solve the master equation for a quasi-monochromatic wavelet around ω_c:

$$\partial_r\Gamma_2+\boxed{i\frac{k_d}{2k_c^2}\Delta_{\perp d}\Gamma_2+k_c^2\left(A(0)-A(r_{\perp d})\right)\Gamma_2}+\boxed{\frac{k_d^2}{2}A(0)\Gamma_2}=0.$$

Diffraction effect — Wandering effect

Initial condition: $\Gamma_2(r\sim 0,t)=\dfrac{1}{4\pi}$ $\qquad$ $\widehat{I}(r\sim 0,t)=\dfrac{1}{4\pi r^2}\delta\left(t-\dfrac{r}{V_0}\right)$

Synthesized spherical envelope in 3-D random media based on the Markov approximation

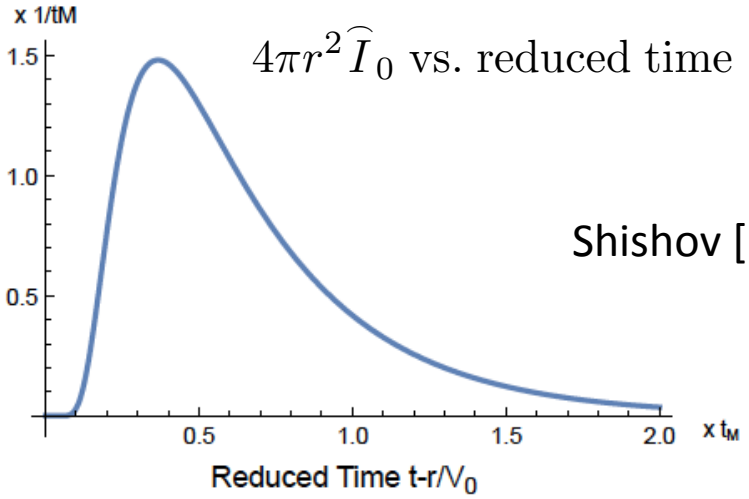

$4\pi r^2 \widehat{I}_0$ vs. reduced time

Shishov [1974]

Gaussian ACF: $R(\mathbf{x}) = \varepsilon^2 \exp[-r^2/a^2]$

Characteristic time of envelope width:

$$t_M = \frac{\sqrt{\pi}\varepsilon^2}{2V_0 a} r^2 \propto r^2$$

$$\widehat{I}_0(r,t,\omega_c) = \frac{1}{4\pi r^2} \frac{\pi^2}{16\, t_M(r)} \vartheta_4'' \left(0, e^{-\frac{\pi^2}{4}\frac{(t-r/V_0)}{t_M(r)}}\right)$$

Elliptic theta func. $\vartheta_4(v,q) = 1 + 2\sum_{n=1}^{\infty} (-1)^n q^{n^2} \cos 2nv$

$$\widehat{I} = \widehat{I}_0 * w$$

Freq. independent

Diffraction effect Wandering effect

$$w(r,t) \propto e^{-\frac{t^2}{t_w(r)^2}}$$

$$t_W = \sqrt{\frac{2\sqrt{\pi}\varepsilon^2 a r}{V_0^2}} \propto \sqrt{r}$$

MS Envelopes of spherical wavelet in von Karman-type Random Media

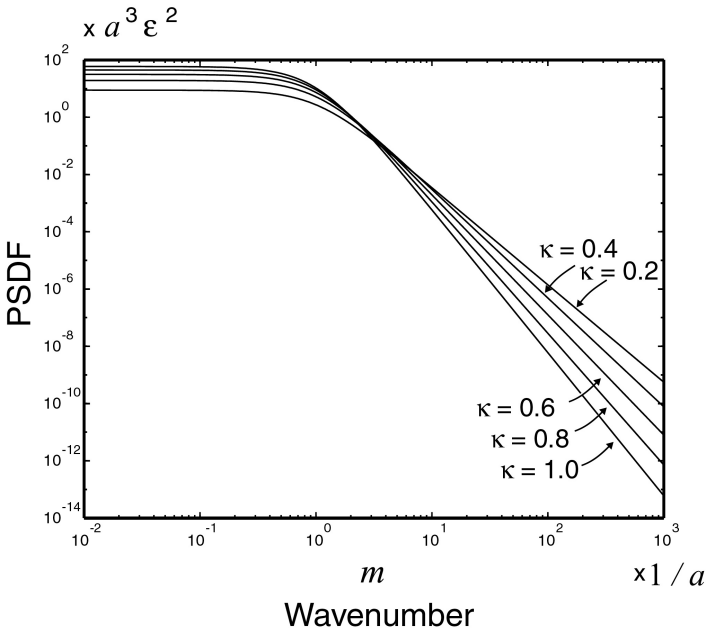

$a\,k_c >> 1$

Saito et al. [2001]

$\widehat{I}_0$ at 100km , ε=0.05, a=5 km

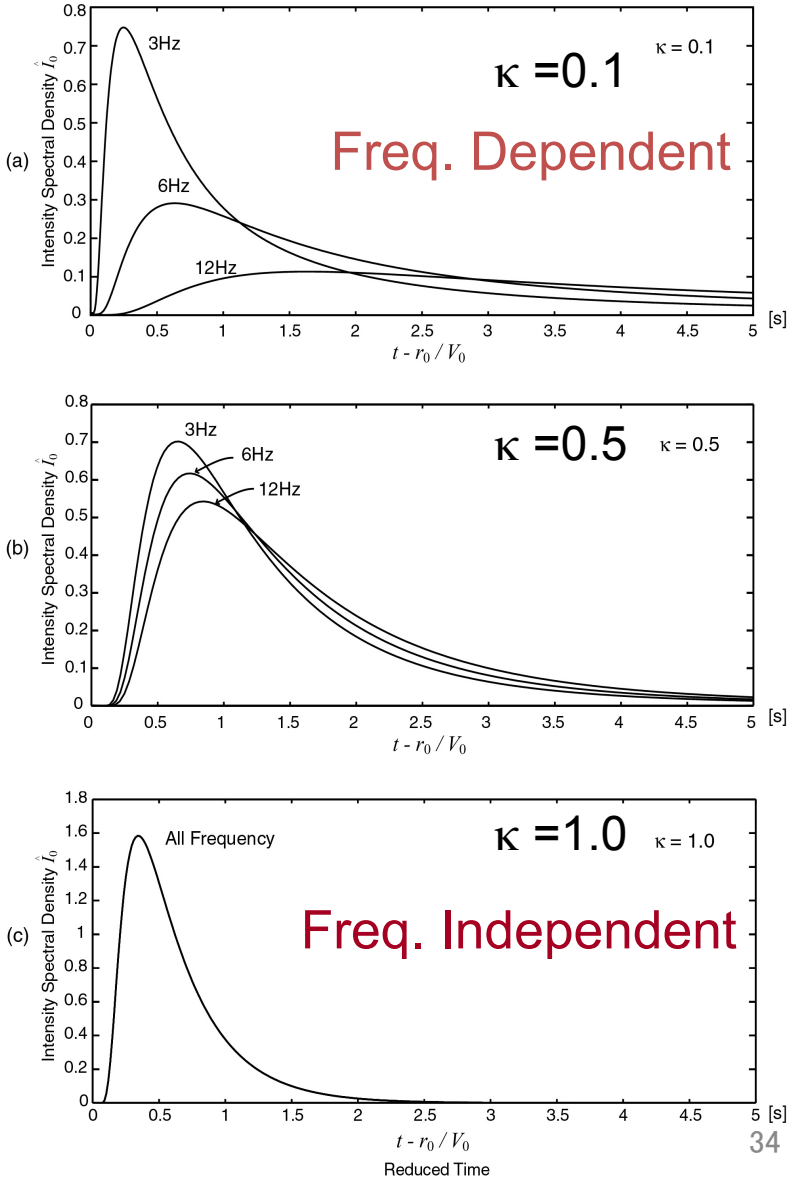

Envelope Broadening of Spherical Scalar Wavelet in 3-D

$\sqrt{\widehat{I}_0}$

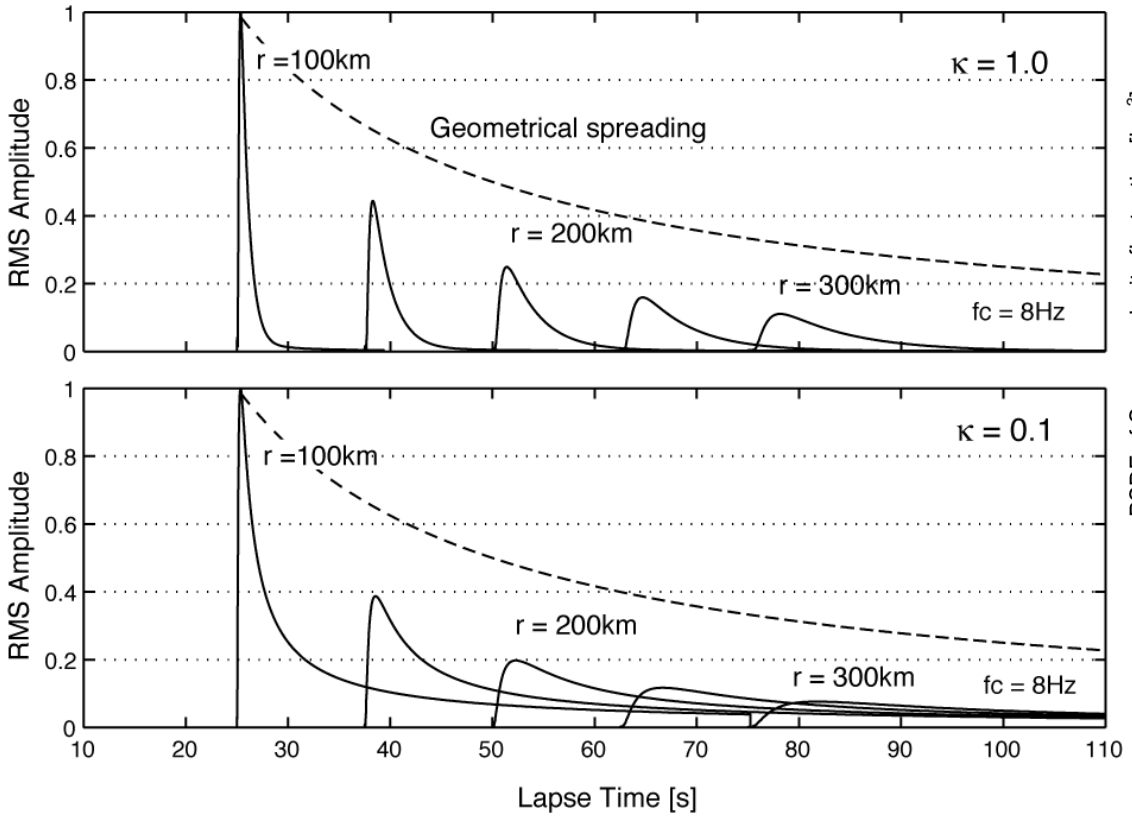

Von Karman-Type

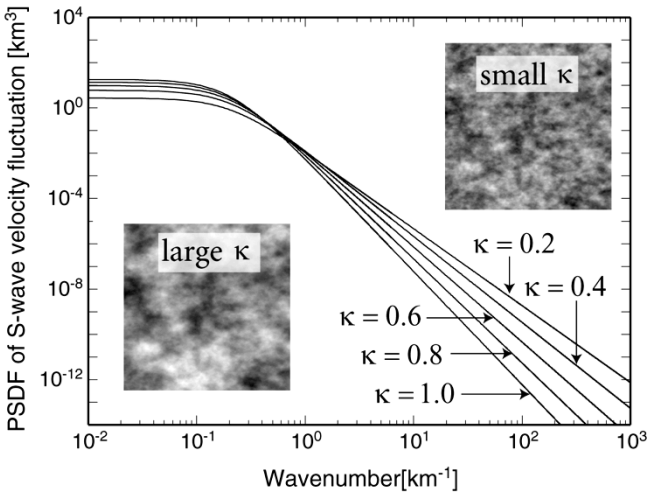

$$P(m) = \frac{8\pi^{3/2}\varepsilon^2 a^3 \Gamma(\kappa + 3/2)}{\Gamma(\kappa)\left(1 + a^2 m^2\right)^{\kappa+3/2}}$$

For an impulsive source radiation, the peak delay from the onset and the envelope width increase with travel distance.

Saito et al. [2001]

Comparison of Markov- and FD-Envelopes in 2-D

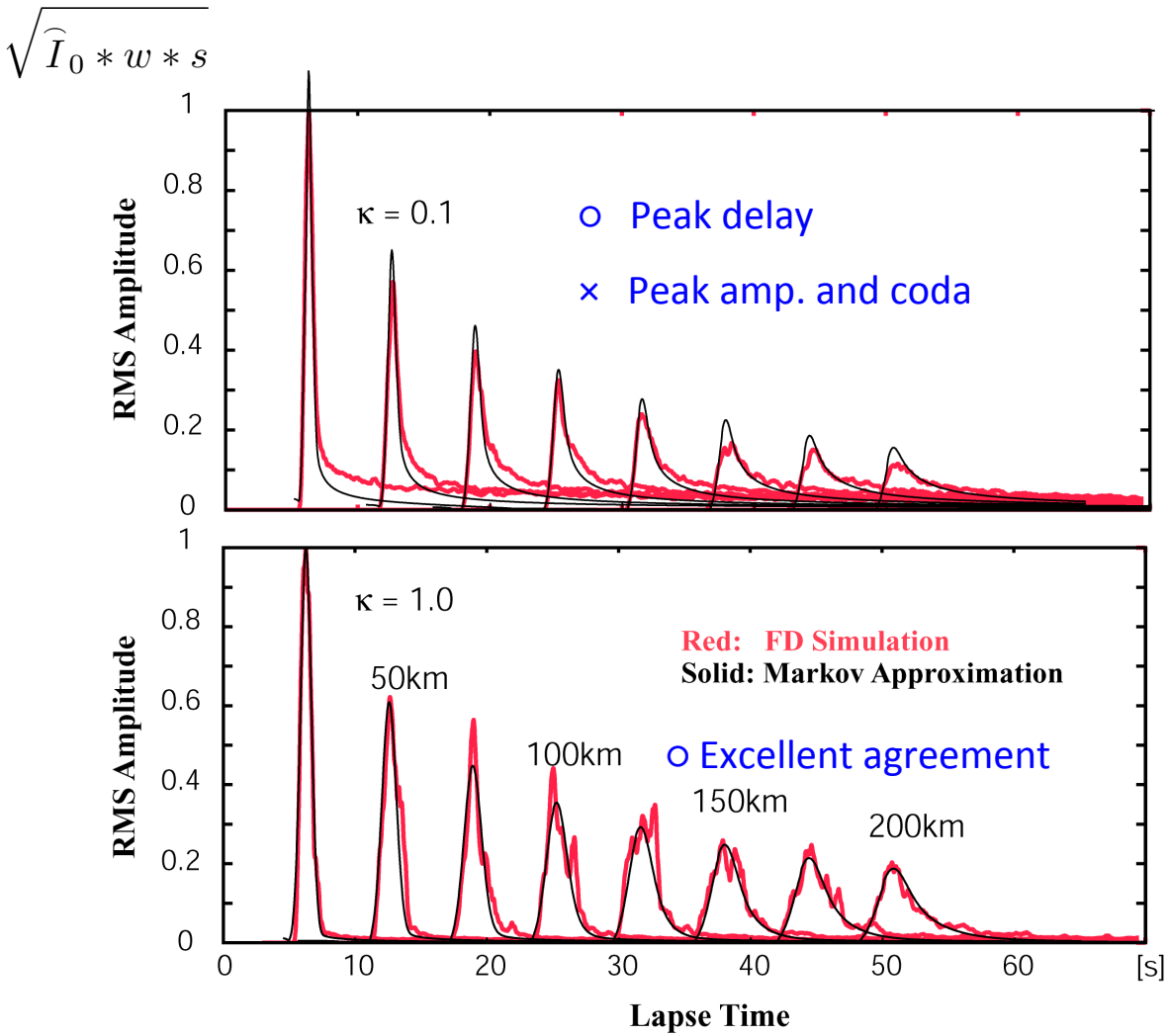

Envelopes of 2Hz Ricker Wavelet in von Karman-Type Random Media

ε=0.05, a=5km

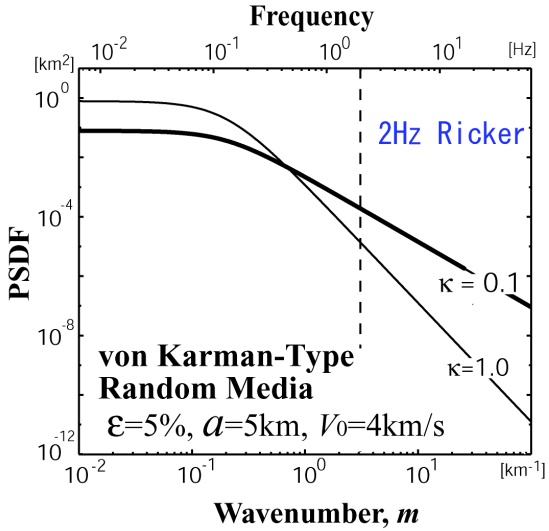

Saito et al. [2003]

Peak delay (t_p) from the S-onset vs. travel distance

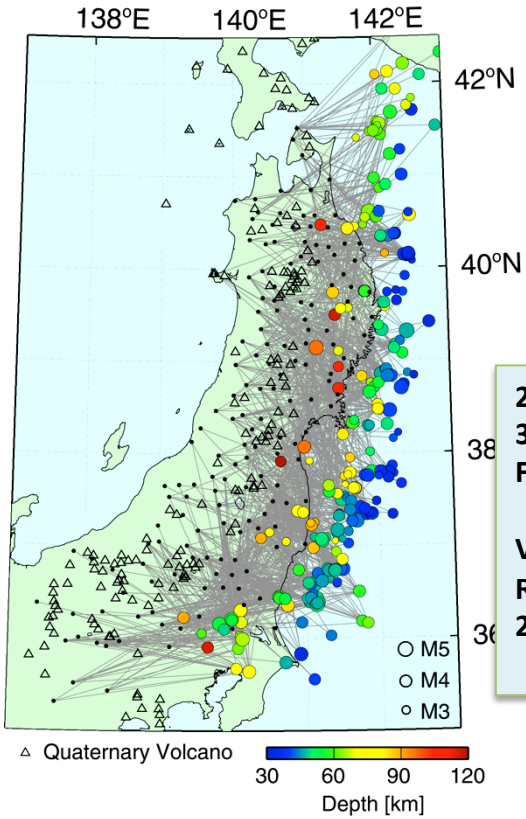

262 Hi-net Stations
326 Earthquakes (M2.3~5.5)
Focal depths > 35 km

Velocity Seismograms
RMS Envelopes (3-comp.)
2~4Hz, 4~8Hz, 8~16Hz, 16~32Hz

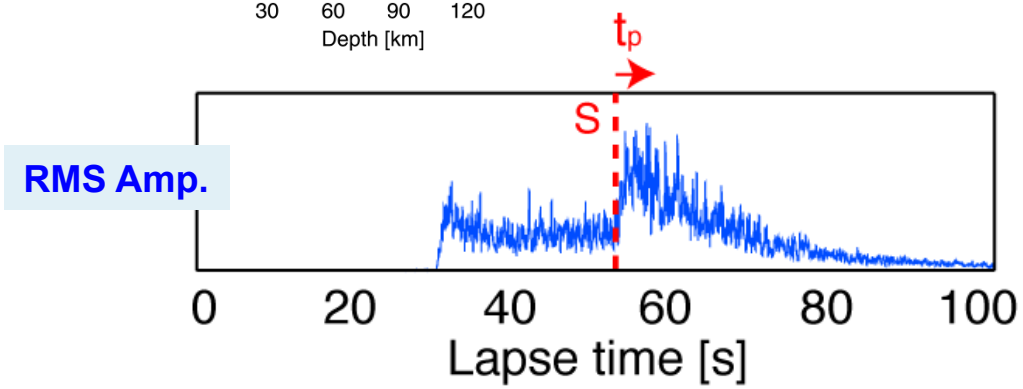

Residual from the regression line means relative strength of scattering along the ray

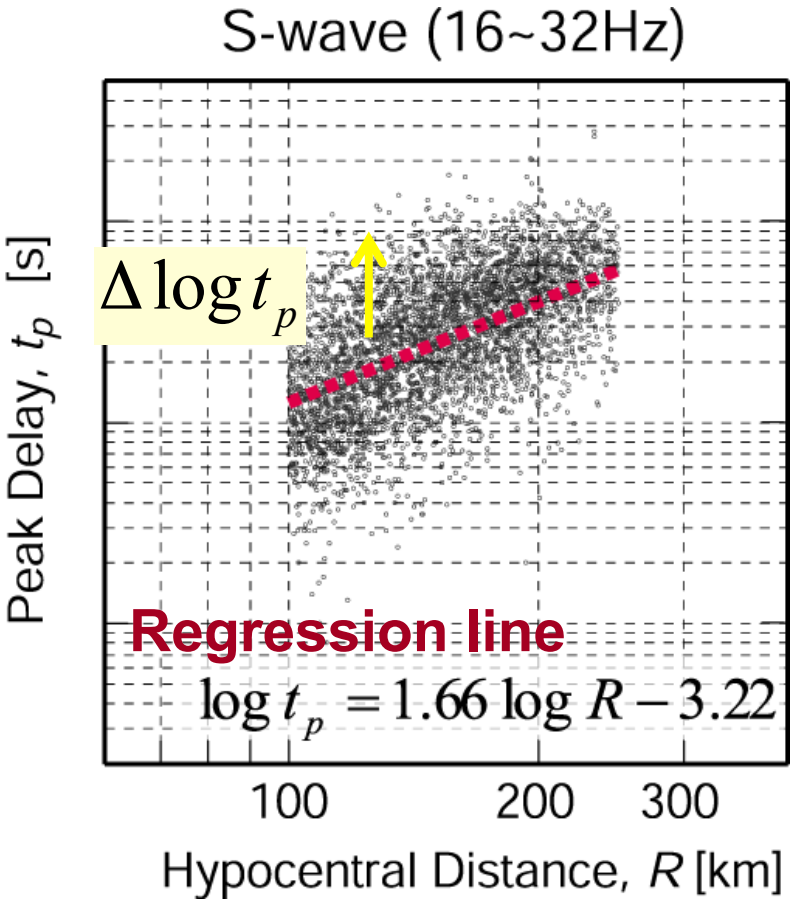

Takahashi et al. [2007]

Peak delay is large for a ray traveling beneath Quaternary volcanoes

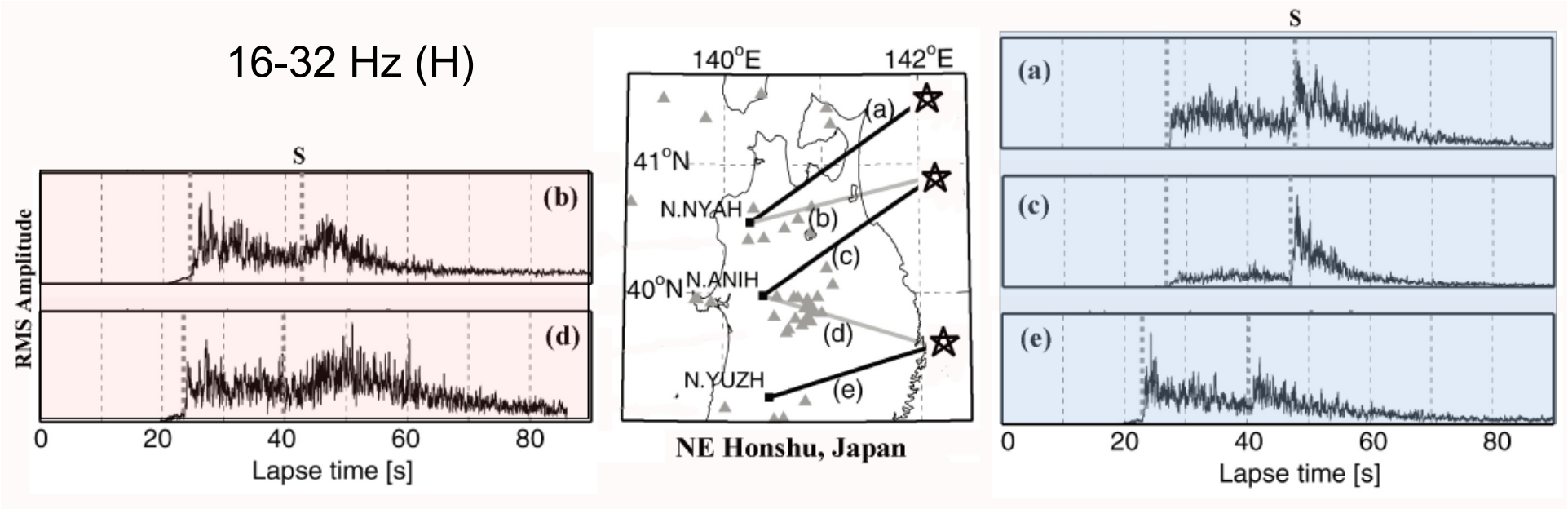

Paths beneath Q. volcanoes

Paths between Q. volcanoes

Strong inhomogeneity beneath Quaternary volcanoes

Takahashi et al. [2007]

Frequency dependence of peak delay in Tohoku, Japan

$$\log\left(\frac{t_p[f]}{t_p[4-8\mathrm{Hz}]}\right) = A_{\mathrm{freq}} + B_{\mathrm{freq}} \log f$$

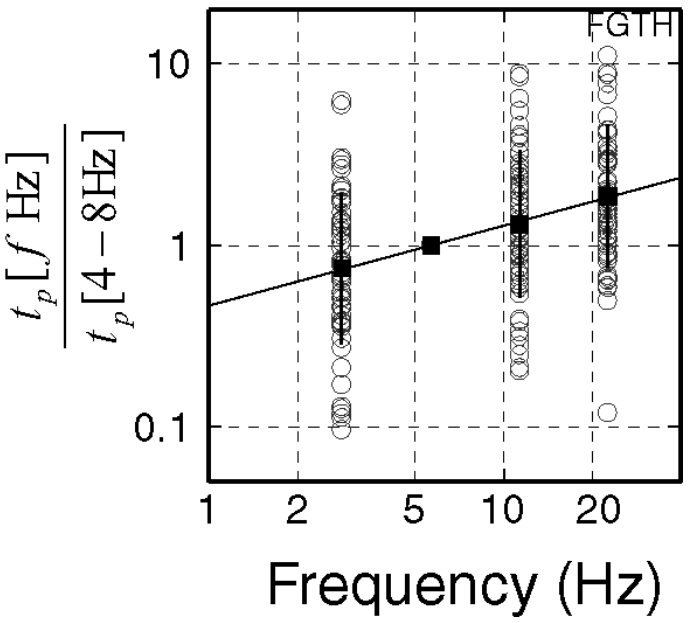

Strong freq. dependence at the back-arc side of the Quaternary Volcanoes.

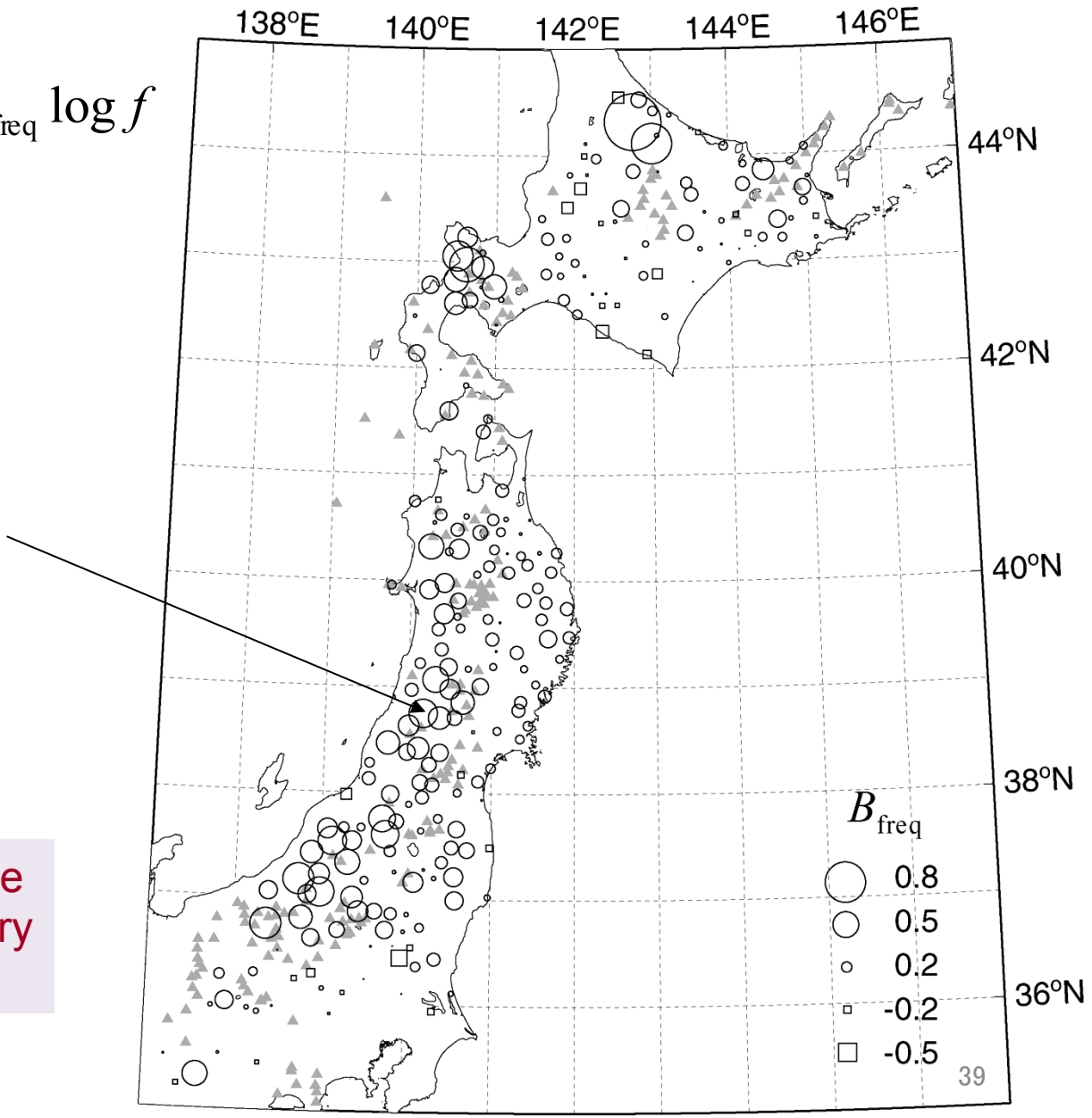

Inversion of PSDF of Velocity Frac. Fluc.

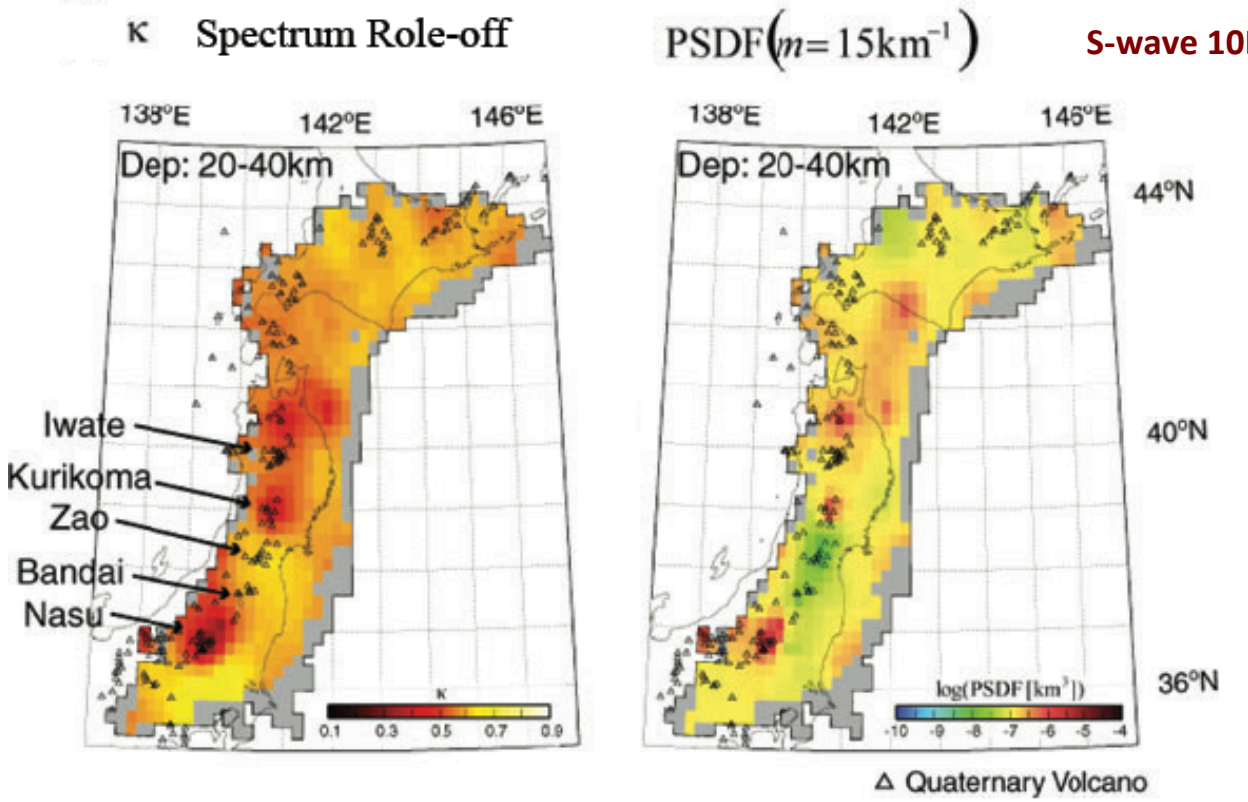

von Karman-type random media

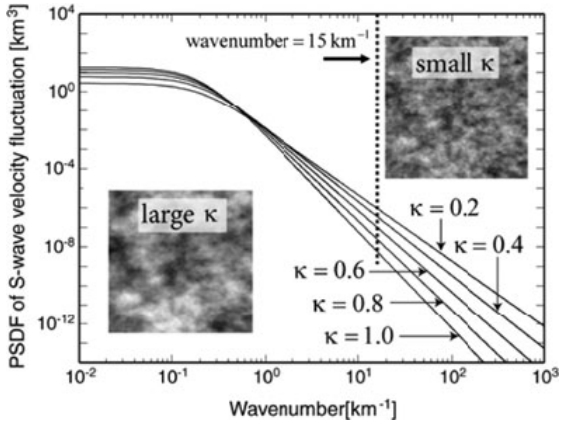

Spectral role-off is small and random inhomogeneity is strong especially beneath Quaternary volcanoes.

Takahashi et al. [2009]

Envelope broadening in Kanto

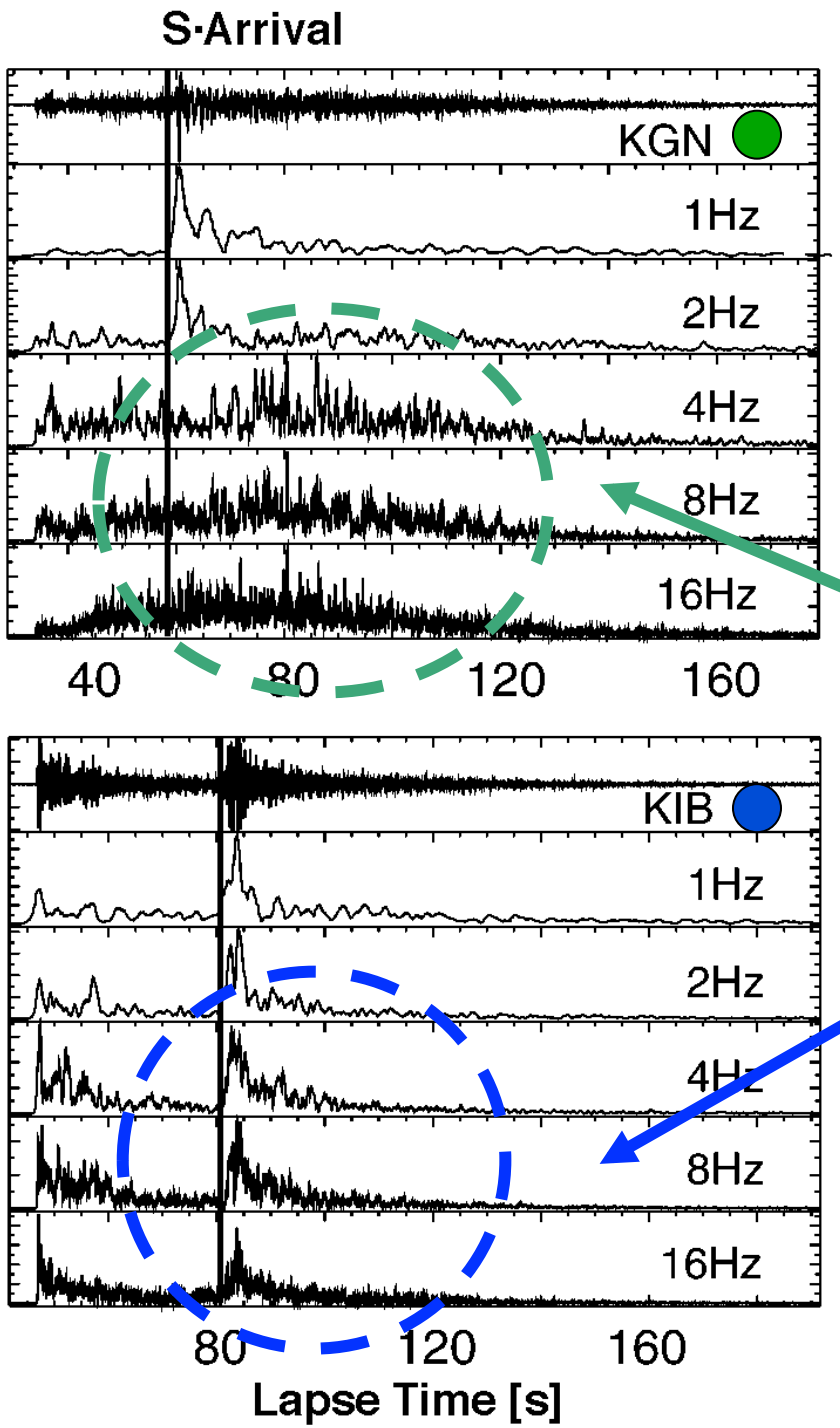

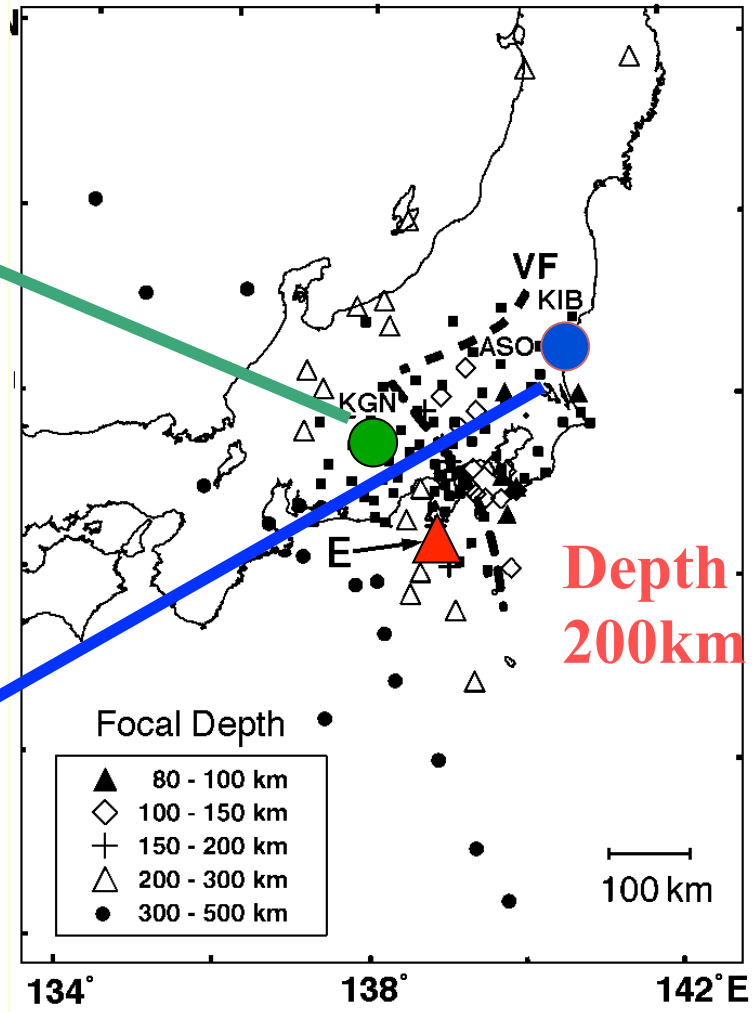

Obara and Sato [1995]

Inhomogeneity beneath the Kanto-Tokai Area, Japan

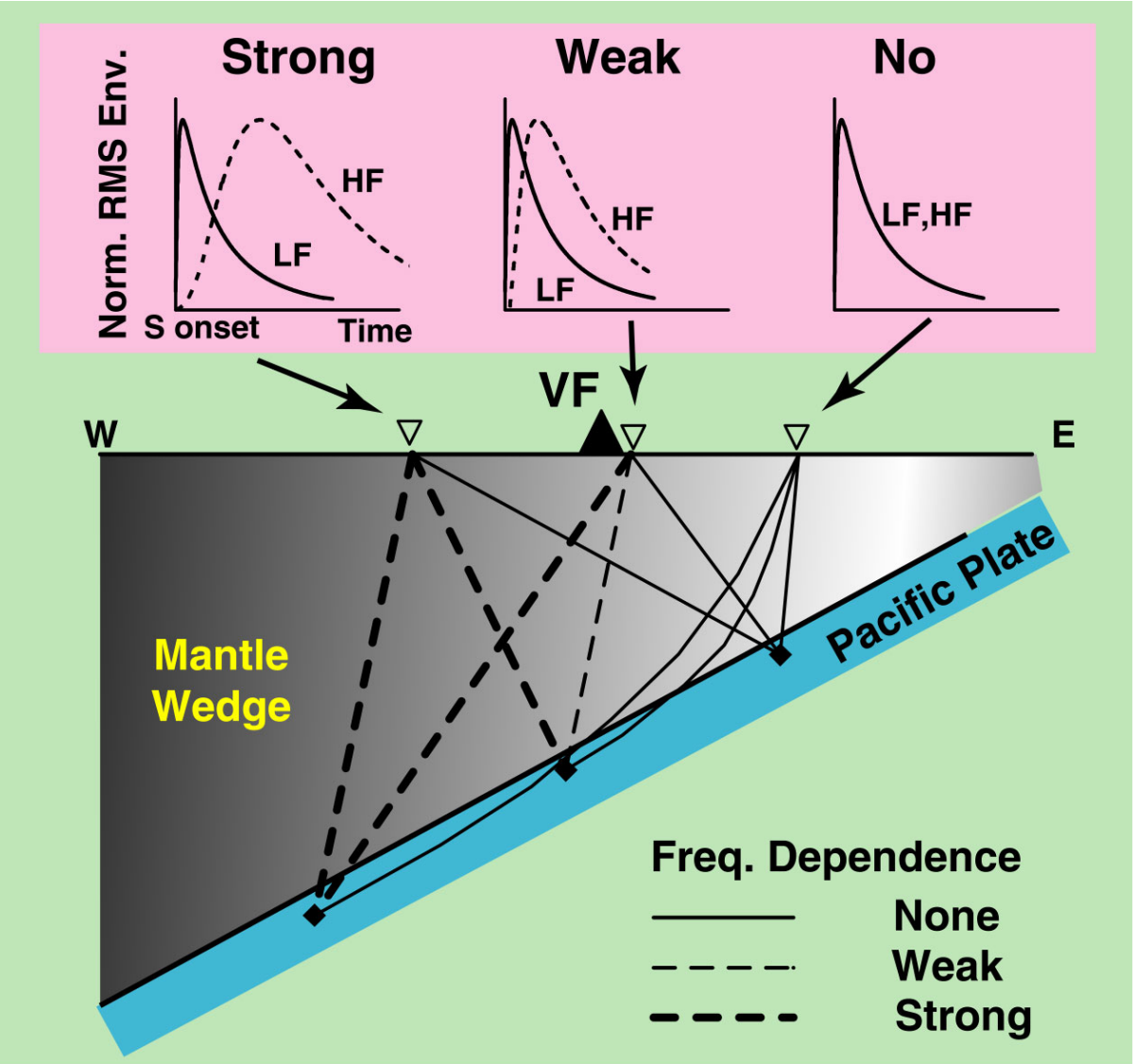

Obara and Sato [1995]

P-Wave Envelopes of Teleseismic Events

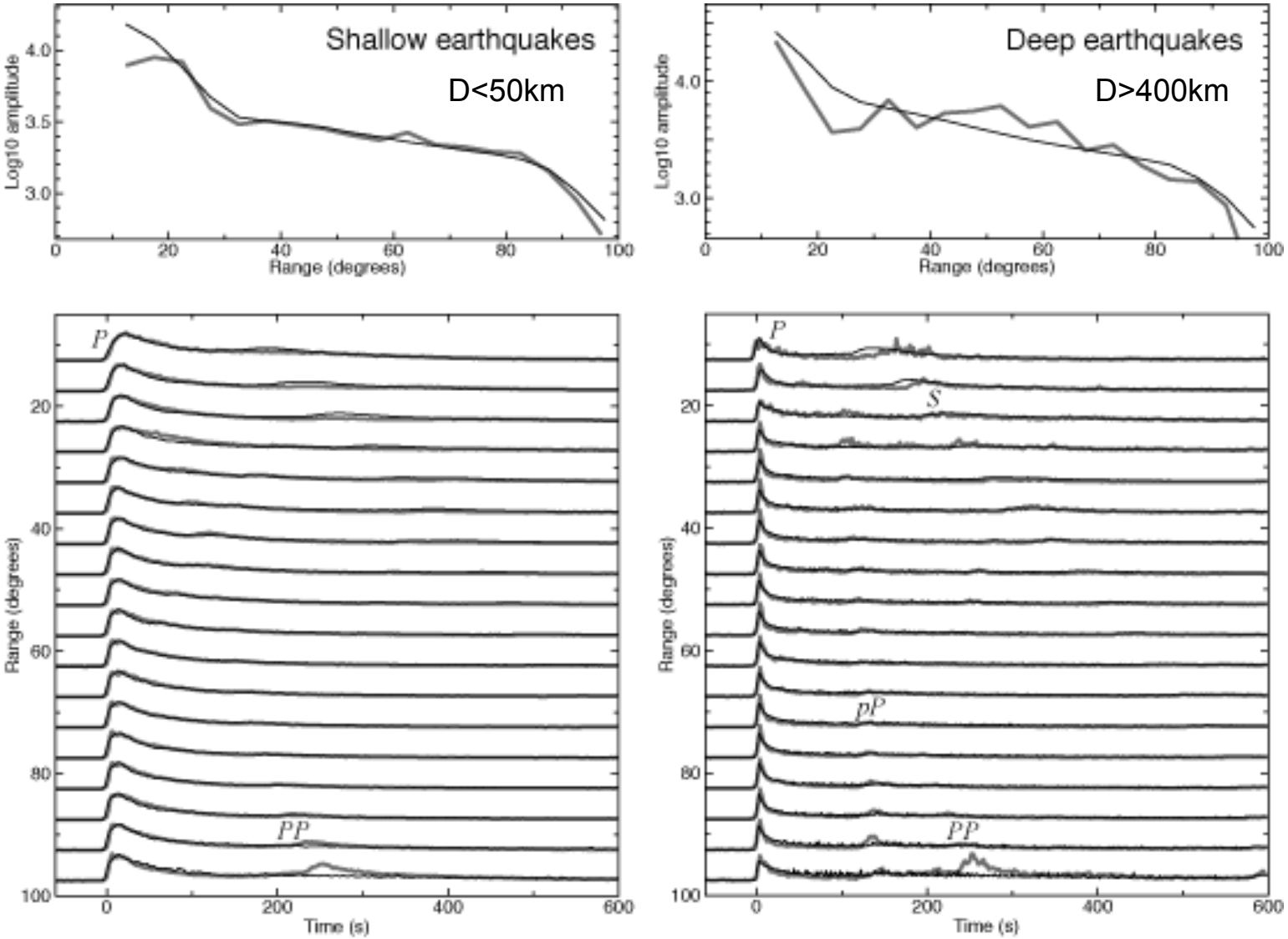

Estimate the randomness from RTT using Born Scattering Amplitudes (f_c ~ 1Hz)

Shearer and Earle [2004]

Energy partition of teleseismic P-wavelet into the transverse component as a measure of lithospheric heterogeneity

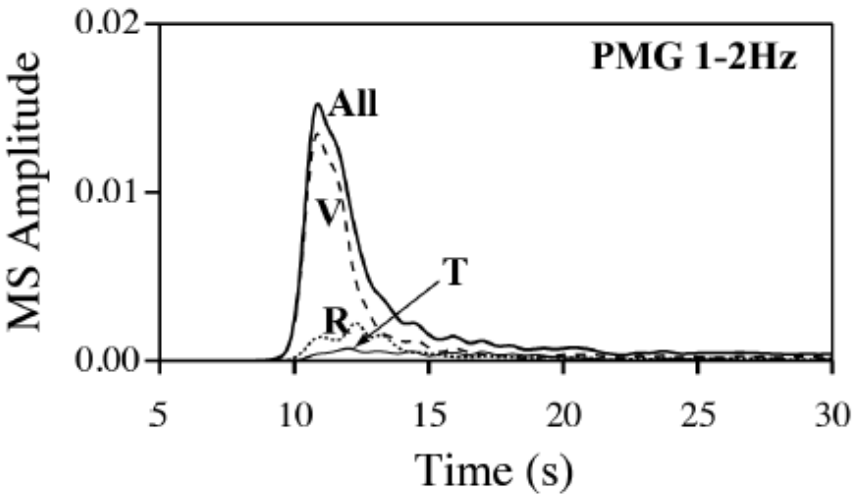

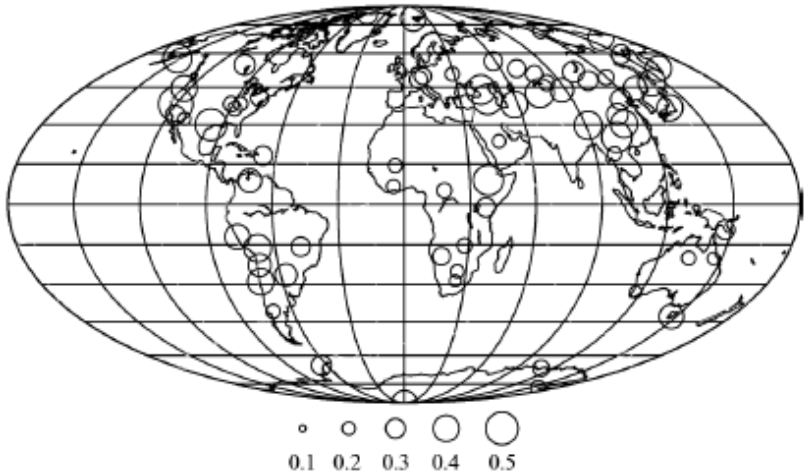

$$\sqrt{\frac{T}{V+R+T}}$$

Kubanza et al. [2006]

Excitation of vertical-component in stacked ScS wavelet envelope

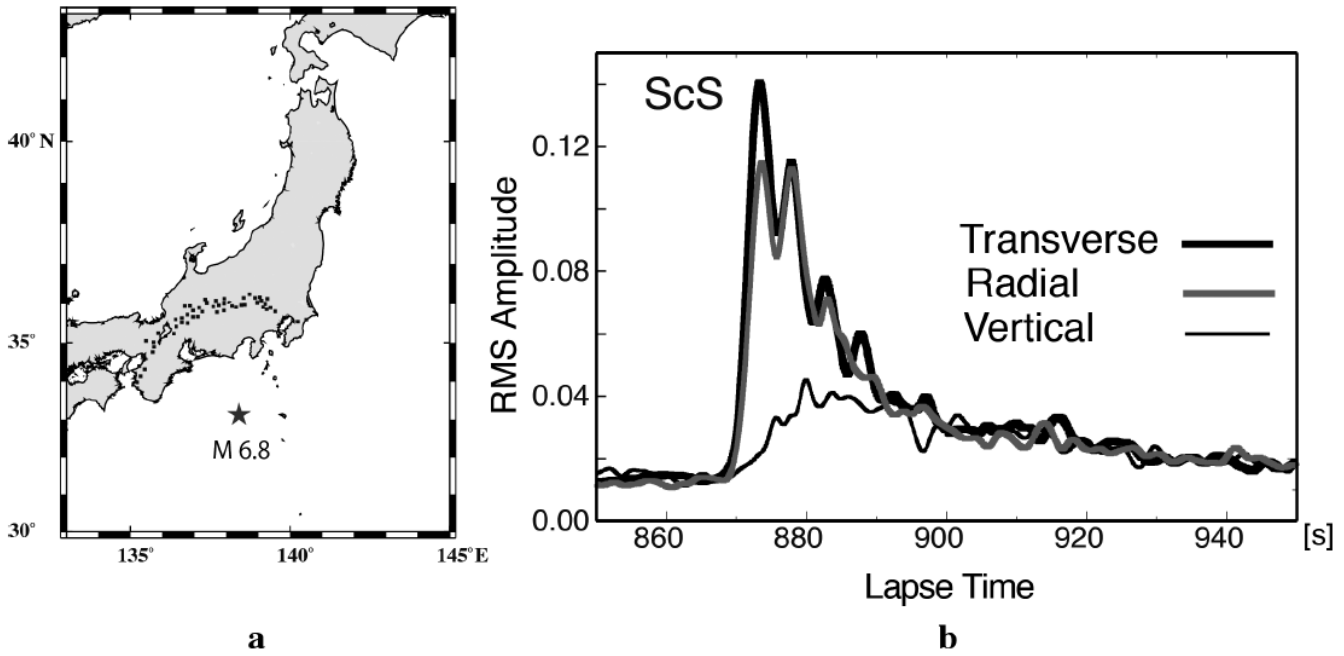

Fig. 9.41 (a) Epicenter (star) of an M 6.8 earthquake with a focal depth of 333 km and 53 Hi-net stations (dots) located within a range of 300 - 350 km in epicentral distance. (b) RMS envelopes around the ScS phase for 0.33 - 0.67 Hz. [Courtesy of K. Emoto]

Summary of Reported PSDF of Velocity Fractional Fluctuation

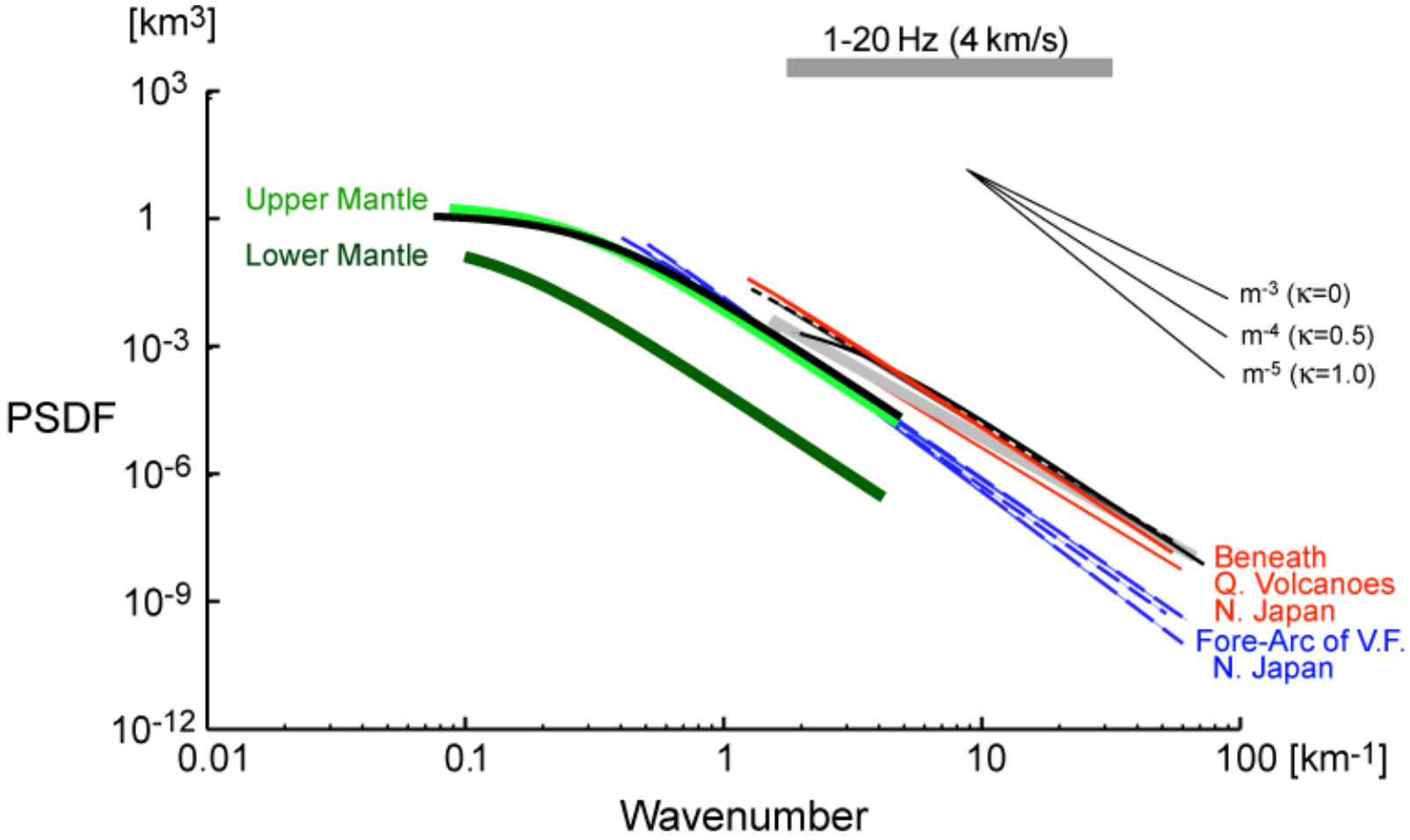

$$V(\mathbf{x}) = V_0\left[1 + \xi(\mathbf{x})\right] \qquad \xi(\mathbf{x}) \Rightarrow P(m)$$

Time lapse movie of
the space distribution of
seismic energy density
of a local earthquake

Hi-net data
Courtesy of K. Emoto

W. Japan
2011/11/21, M 5.2

Semi-log plot of Energy density vs. distance

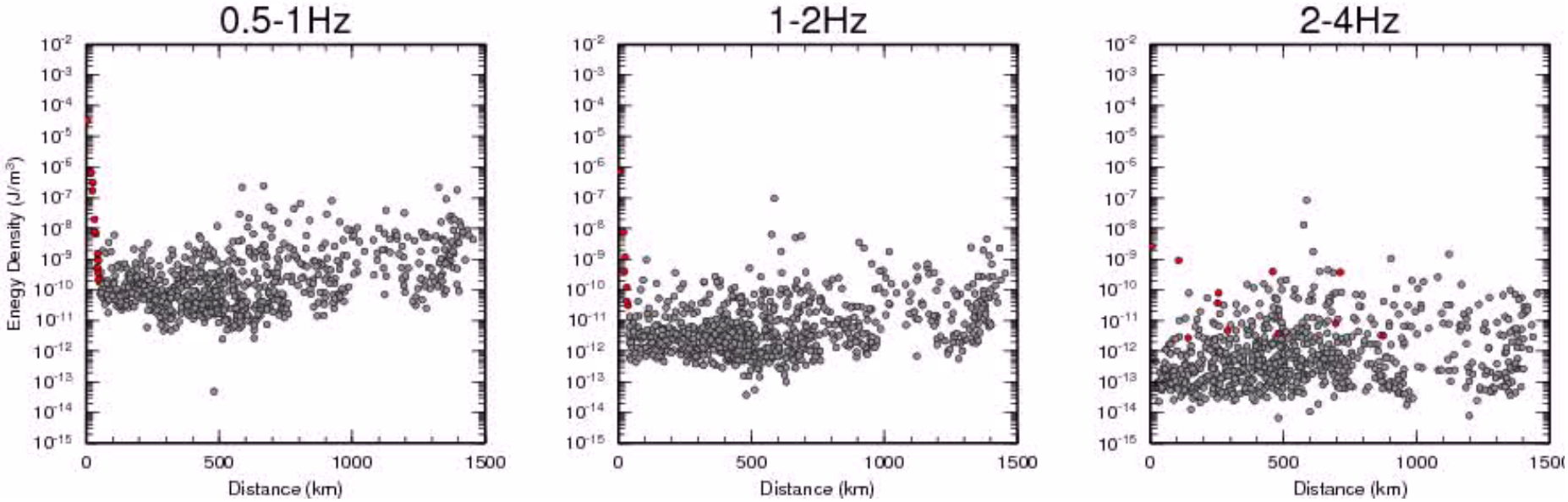

Snap shot of the space distribution of seismic energy（4-8 Hz）[Asano and Saito, 2011]

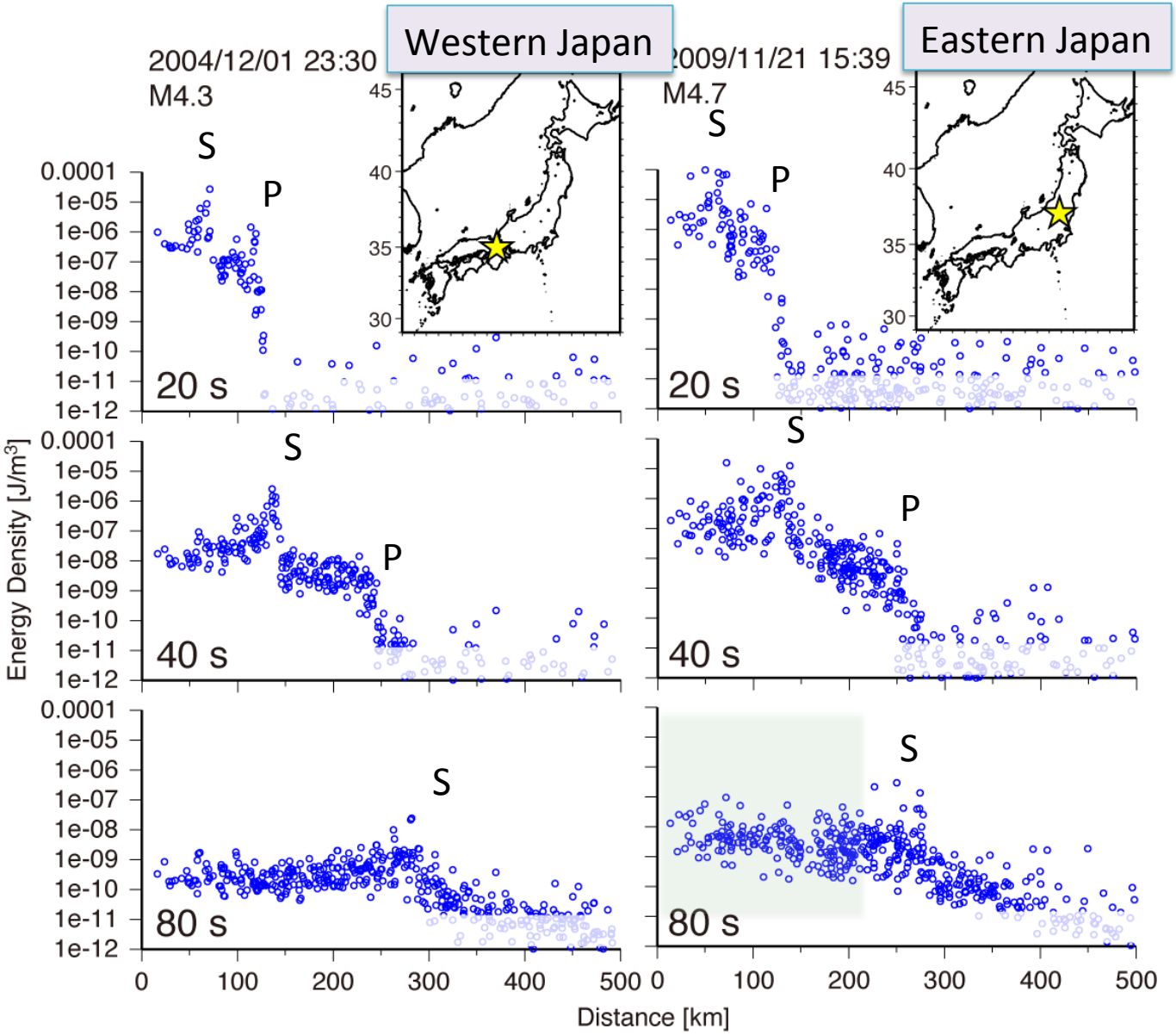

For von-Karmann-type random media, $k_c >> a^{-1}$ means the power-law range, where k_c^{-1} is the unique scale of length.

To apply strictly the parabolic approximation for slowly varying fluctuations ξ_L :

$$2ik_c\partial_r U + \Delta_\perp U - 2k_c^2\xi_L\left(k_c, \mathbf{x}\right)U = 0$$

$$\partial_r\Gamma_2 + i\frac{k_d}{2k_c^2}\Delta_{\perp d}\Gamma_2 + k_c^2\left(A_L\left(0\right) - A_L\left(r_{\perp d}\right)\right)\Gamma_2 + \frac{k_d^2}{2}A_L\left(0\right)\Gamma_2 = 0, \qquad A_L\left(r_\perp\right) \equiv 2\int_0^\infty dz\, R_L\left(\boldsymbol{x}_\perp, z\right)$$

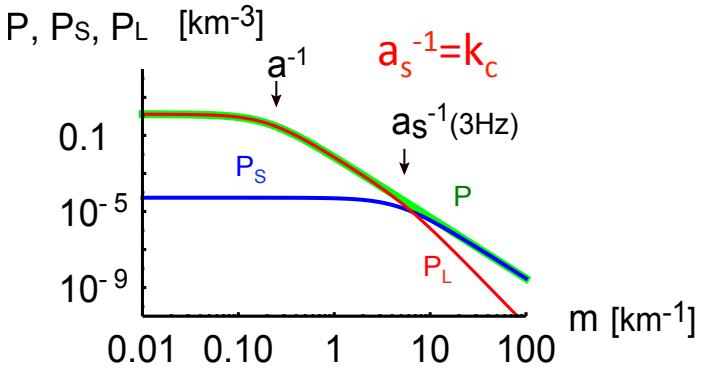

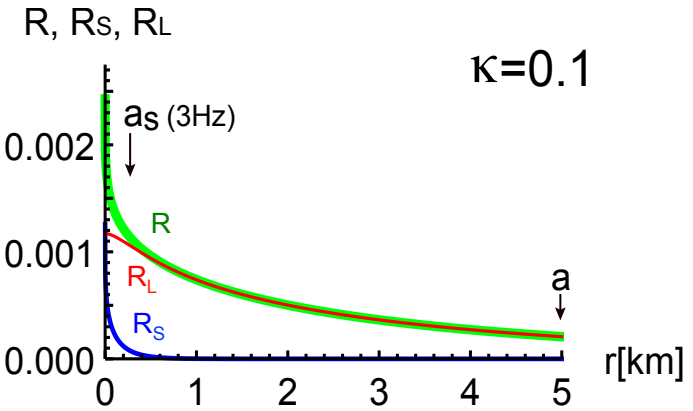

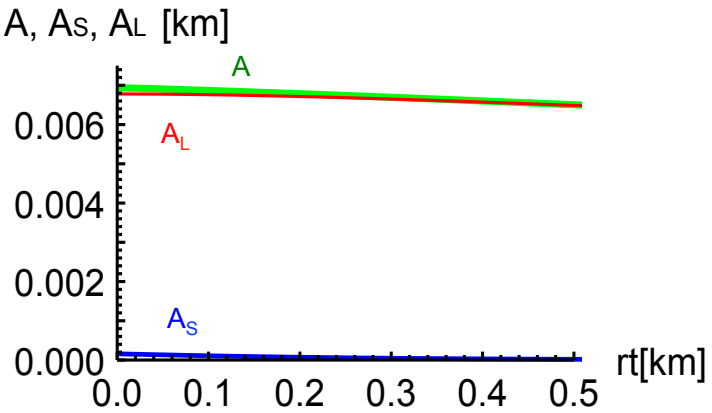

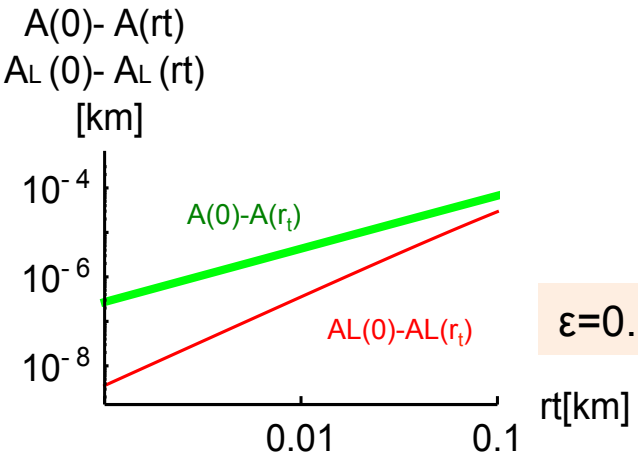

ε=0.05, a=5km

$$G_{M0}(\boldsymbol{x}, t, \omega_c) = \frac{1}{4\pi r^2 V_0} \frac{\pi^2}{16\, t_M} \vartheta_4'' \left(0, e^{-\frac{\pi^2}{4}\frac{(t-r/V_0)}{t_M}}\right)$$

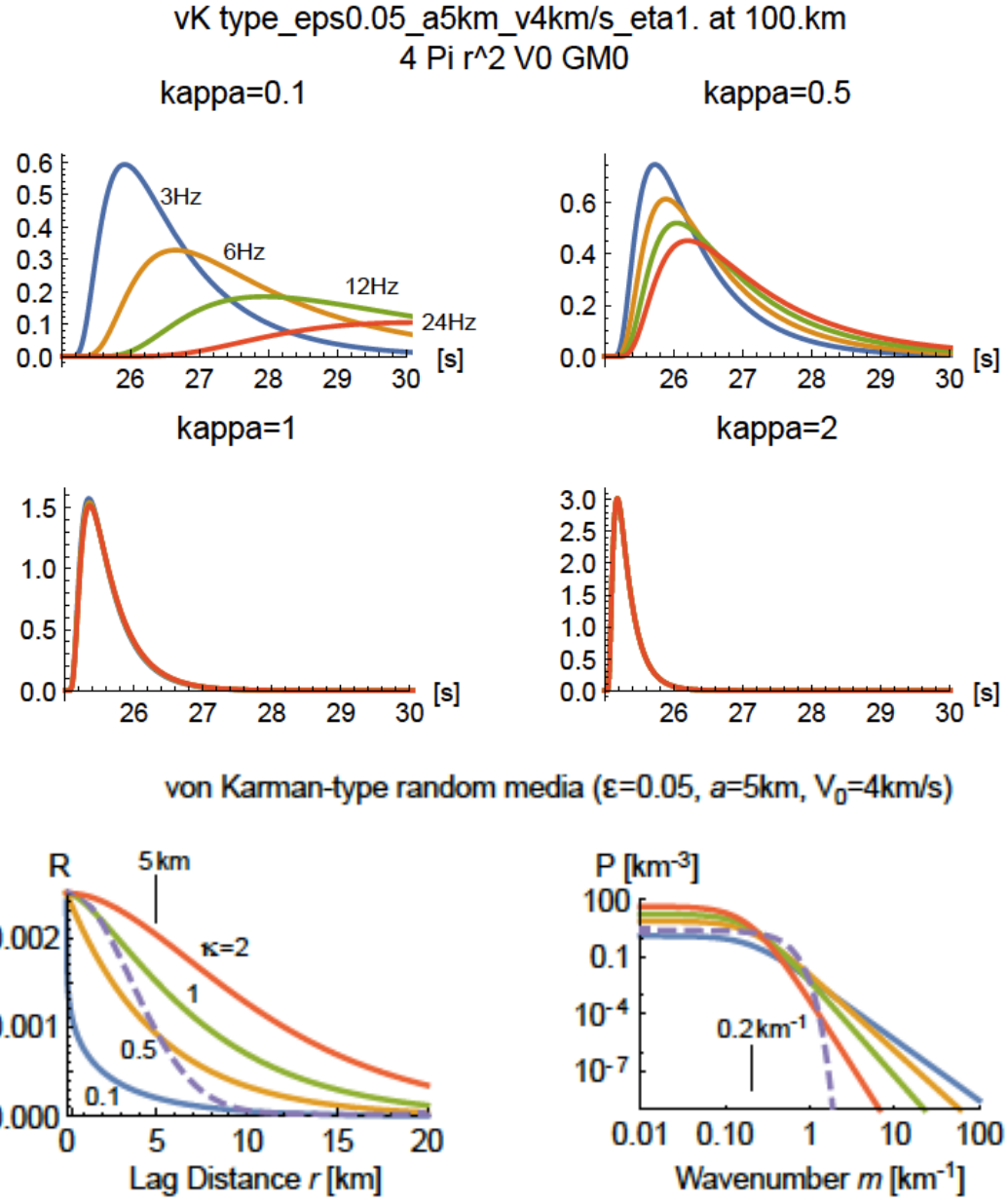

$4\pi r^2 V_0 G_{M0}$ vs. reduced time

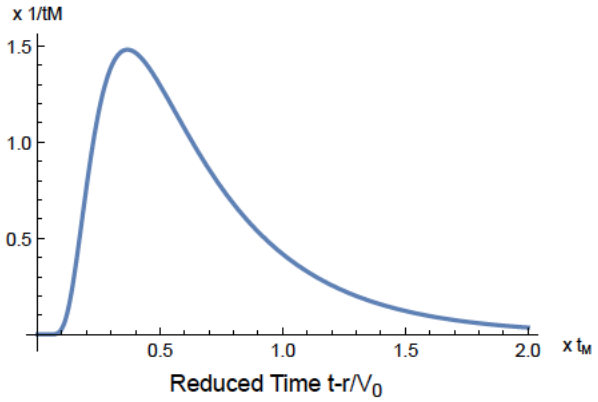

von Karman-type random media (ε=0.05, *a*=5km, V_0=4km/s)

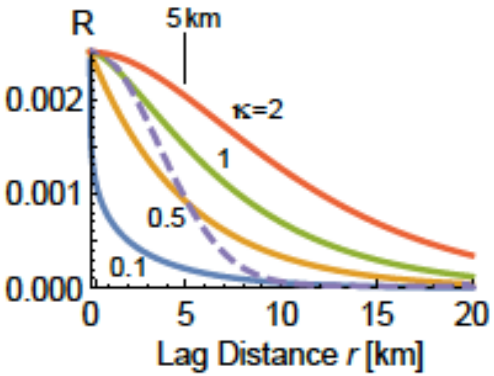

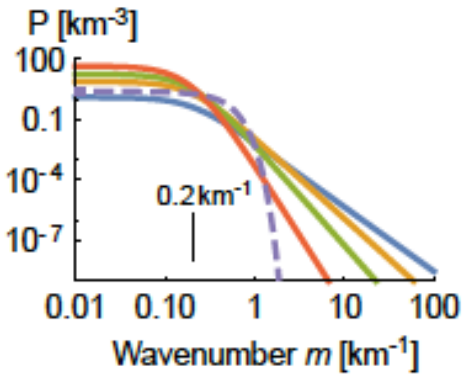

Broadening and wandering

$t_M(\kappa, r, f_c)$ and $t_W(\kappa, r, f_c)$

at 100km

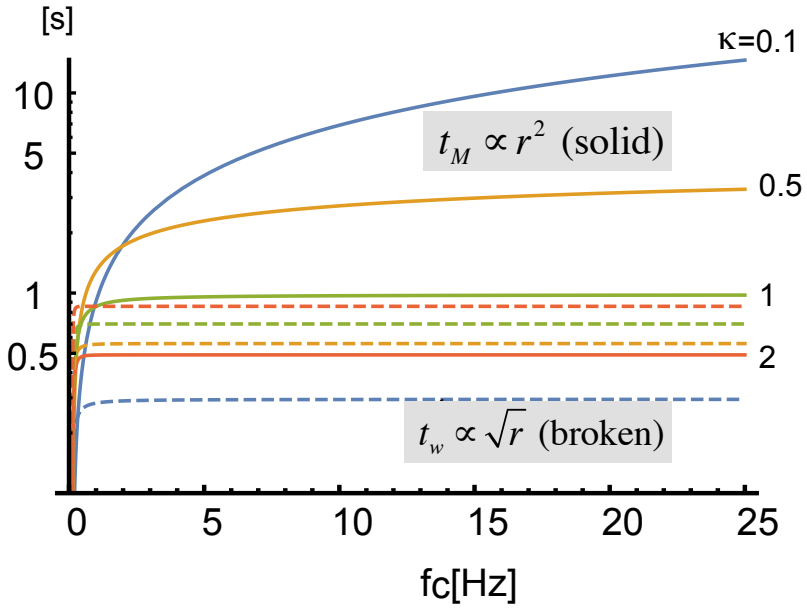

TrSC

$$g_m(\kappa, f_c) = \frac{1}{4\pi}\int_0^{2k_c} P(m) m^3 \, dm$$

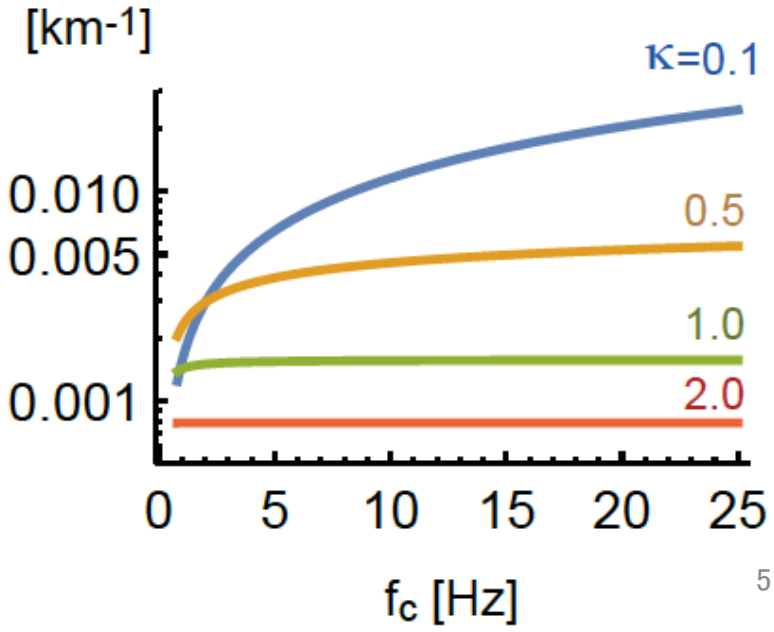

Multiple isotropic scattering model using the Markov propagator and TrSC

$$G_{M0}(\boldsymbol{x},t,\omega_c)=\frac{1}{4\pi r^2 V_0}\frac{\pi^2}{16\,t_M}\vartheta_4''\left(0,e^{-\frac{\pi^2}{4}\frac{(t-r/V_0)}{t_M}}\right)$$

$$t_M(\kappa,r,\omega_c) \text{ and } t_W(\kappa,r,\omega_c)$$

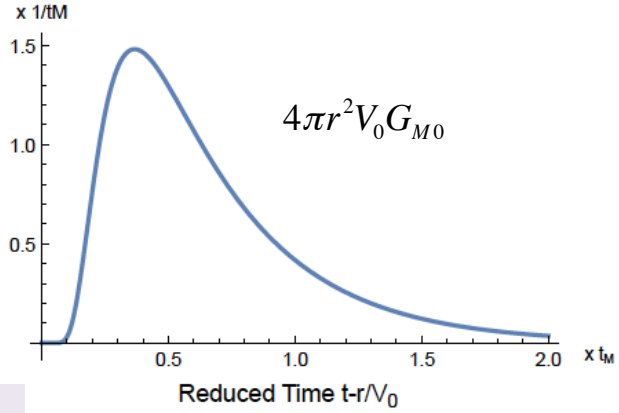

Markov propagator=diffraction + wandering + scattering loss

$$G_M = G_{M0} * w$$

$$G_M^S(\mathbf{x},t;\omega_c)=G_M(\mathbf{x},t;\omega_c)e^{-V_0 g_m(\omega_c)t}$$

$$E(\mathbf{x},t;\omega_c)=G_M^S(\mathbf{x},t;\omega_c)+V_0\,g_m(\omega_c)\int_{-\infty}^{\infty}G_M^S(\mathbf{x}-\mathbf{x}',t-t';\omega_c)E(\mathbf{x}',t';\omega_c)\,dt'd\mathbf{x}'$$

TrSC (Effective isotropic scat. co.): $g_m(\kappa,\omega_c)=\frac{1}{4\pi}\int_0^{2k_c}P(m)m^3\,dm$

Correct to satisfy the energy conservation: $E_c(\mathbf{x},t;\omega_c)=\frac{E(\mathbf{x},t;\omega_c)}{\int E(\mathbf{x},t;\omega_c)\,d\mathbf{x}}$

$$4\pi r^2 V_0\int G_{M0}(\mathbf{x},t,\omega_c)\,dt=1,\qquad \int E_c(\mathbf{x},t,\omega_c)\,d\mathbf{x}=1$$

G_{M0} and E_c

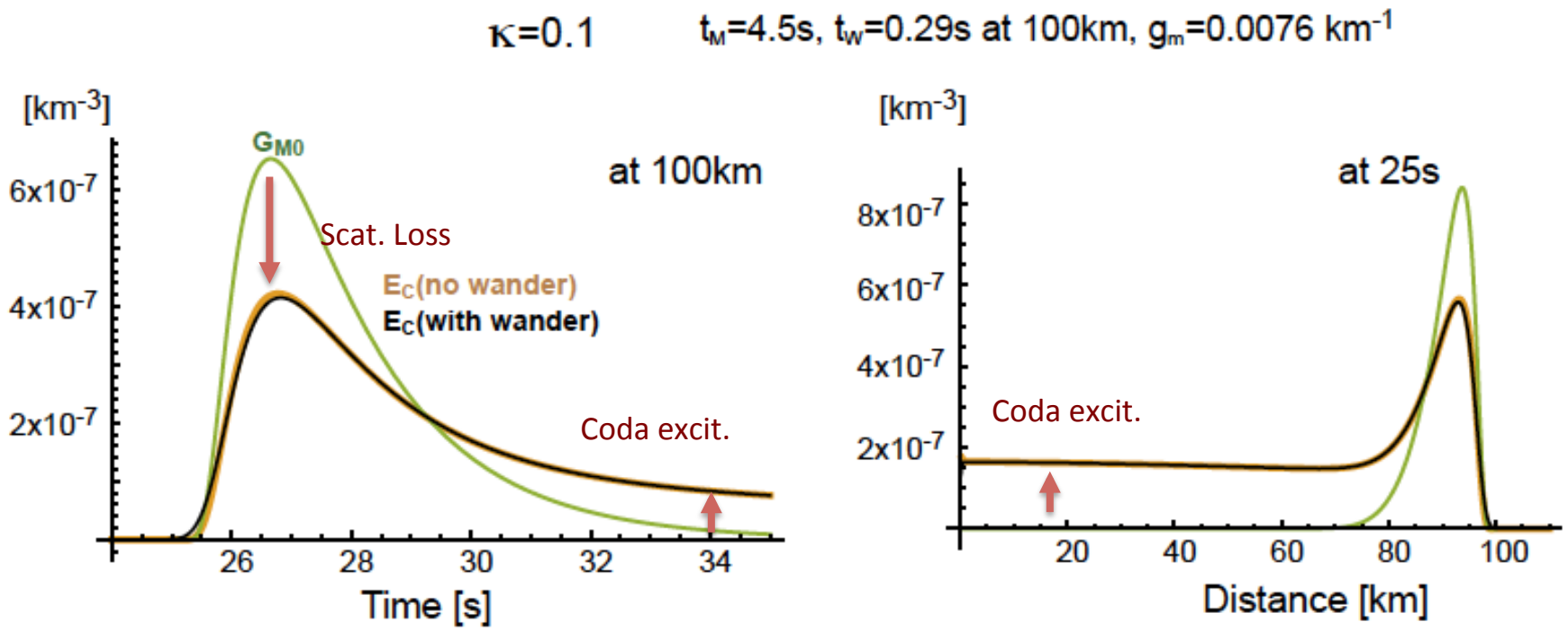
κ=0.1
t_M=4.5s, t_W=0.29s at 100km, g_m=0.0076 km^{-1}
[km^{-3}]
G_{M0}
at 100km
Scat. Loss
E_C(no wander)
E_C(with wander)
Coda excit.
6x10^{-7}
4x10^{-7}
2x10^{-7}
26
28
30
32
34
Time [s]
[km^{-3}]
at 25s
8x10^{-7}
6x10^{-7}
4x10^{-7}
2x10^{-7}
Coda excit.
20
40
60
80
100
Distance [km]

Linear plot of the time- and space-distribution of $E_c(r,t)$

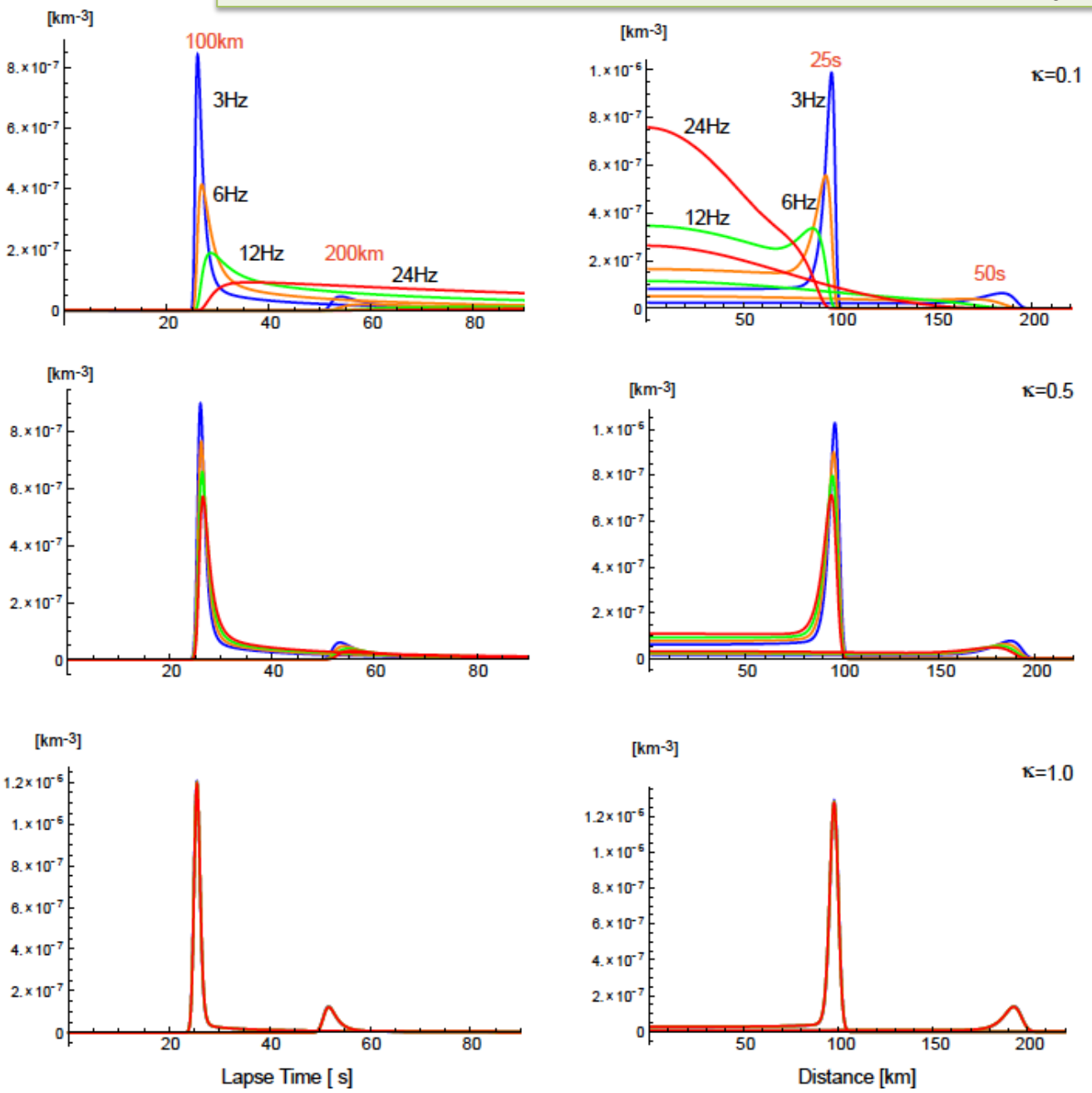

Freq. dependent
Large coda
Strong scattering loss

Freq. independent
Weak coda

Log-log plot of the time- and space-distribution of $E_c(r,t)$

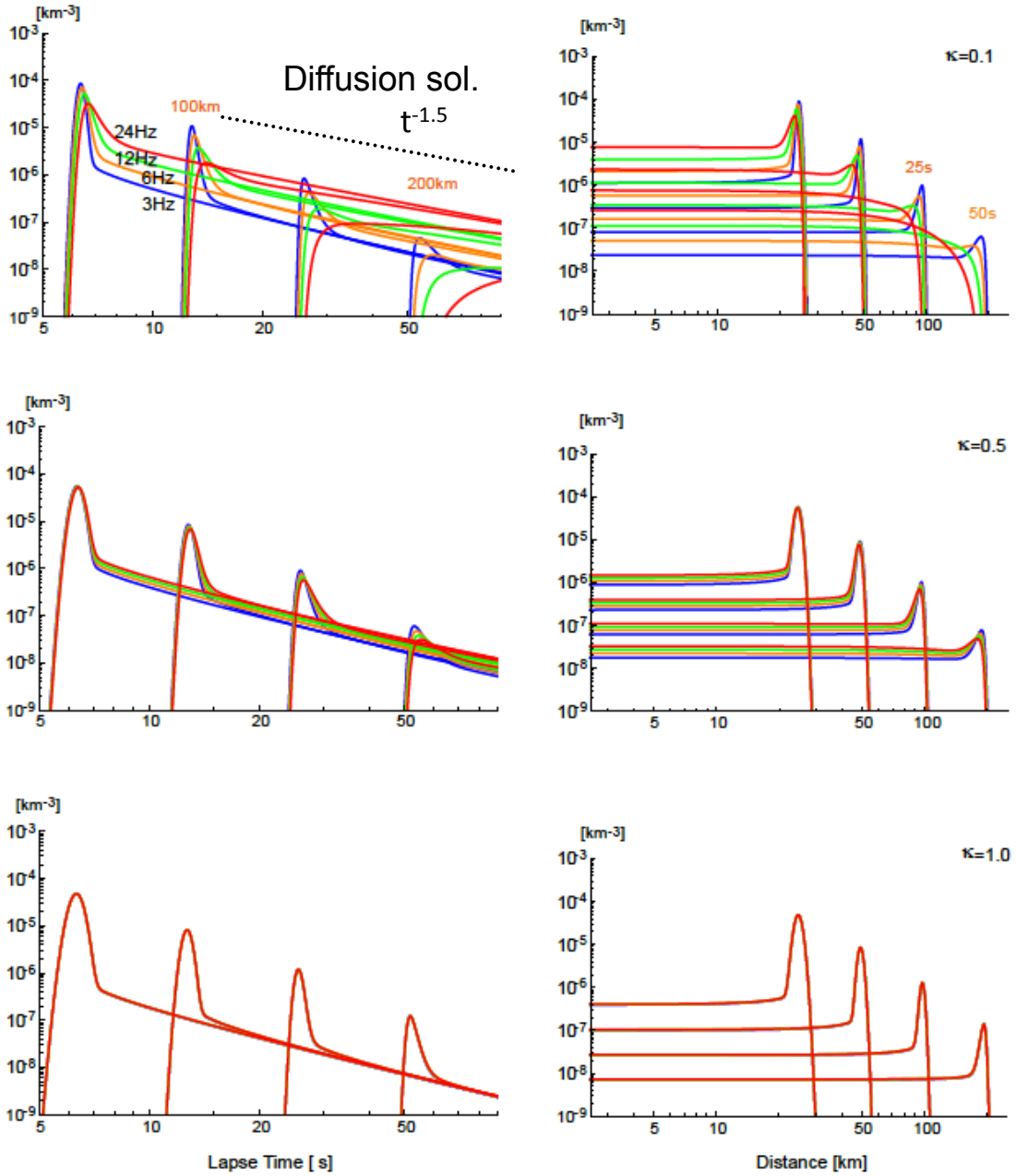

Freq. dependent
Large coda
Strong scattering loss

Freq. independent
Weak coda

Future Studies

- Observation
  - Analysis of whole envelope from P-onset to S-coda
  - Regional differences in scattering characteristics in relation with tectonic settings
  - Measurements of the PSDF of random velocity fluctuation

- Theory
  - Comparison of the RTT solution with FD wave-simulations in 3-D random media having power law spectra
  - Introduction of depth dependence and regional differences in the envelope synthesis
  - Extension of RTT for elastic vector-wave envelopes

References

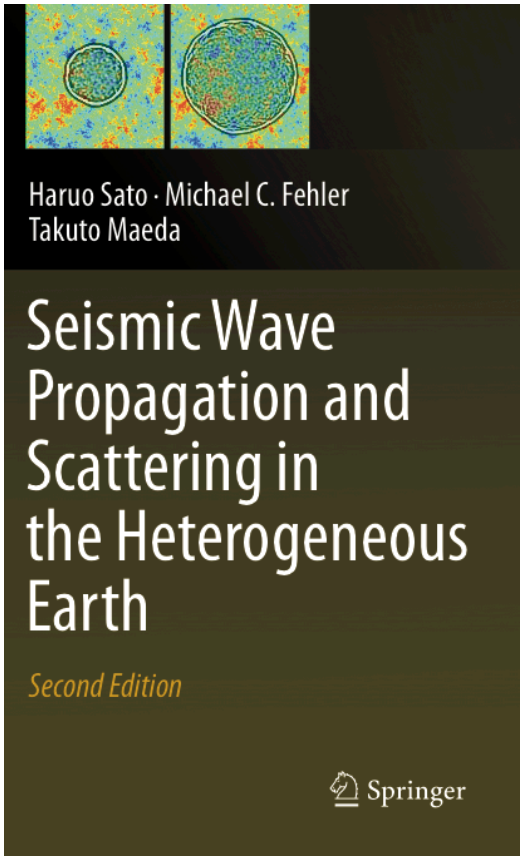

- Bridge between Boltzmann eq. and Stochastic wave theory in random media: Howe [1974], Ryzhik et al. [1996], Margerin [2005].
- RTT of elastic waves through the distribution of spherical obstacles: Margerin et al. [2000].
- Monte Carlo simulation of the Boltzmann eq.: Gusev and Abubakirov [1996], Sens-Schonfelder et al. [2009].
- RTT vs. FD simulation of waves in random media: Frankel and Clayton [1986], Przybilla and Korn [2008], Przybilla et al [2006].
- Markov app. v.s. FD simulation of waves in random media: Fehler et al. [2000], Emoto et al. [2010, 2011].
- Use of RTT solution as a kernel for in the time lapse change measurement of medium parameters: Pacheco and Snieder [2005], Obermann et al. [2013].
- Use of RTT solution for the inversion of source energy radiation: Nakahara et al. [1998], Nakahara [2008]
- Fractal scattering model for the power law decay of amplitude: Sato and Fukushima [2013].

Sato, Fehler and Maeda, "Seismic wave propagation and scattering in the heterogeneous earth: the 2nd edition", Springer, 2012.

http://zisin.geophys.tohoku.ac.jp/~sato/satoHP2012/Information.html